MIT Open Access Articles

A coupled theory of fluid permeation and large deformations for elastomeric materials

A coupled theory of fluid permeation and large deformations for elastomeric materials

Shawn A. Chester and Lallit Anand*
Department of Mechanical Engineering
Massachusetts Institute of Technology
Cambridge, MA 02139, USA

July 26, 2011

Abstract

An elastomeric gel is a cross-linked polymer network swollen with a solvent (fluid). A continuum-mechanical theory to describe the various coupled aspects of fluid permeation and large deformations (e.g., swelling and squeezing) of elastomeric gels is formulated. The basic mechanical force balance laws and the balance law for the fluid content are reviewed, and the constitutive theory that we develop is consistent with modern treatments of continuum thermodynamics, and material frame-indifference. In discussing special constitutive equations we limit our attention to isotropic materials, and consider a model for the free energy based on a Flory-Huggins model for the free energy change due to mixing of the fluid with the polymer network, coupled with a non-Gaussian statistical-mechanical model for the change in configurational entropy — a model which accounts for the limited extensibility of polymer chains. As representative examples of application of the theory, we study (a) three-dimensional swelling-equilibrium of an elastomeric gel in an unconstrained, stress-free state; and (b) the following one-dimensional transient problems: (i) free-swelling of a gel; (ii) consolidation of an already swollen gel; and (iii) pressure-difference-driven diffusion of organic solvents across elastomeric membranes.

Keywords: A. Gels B. Elastomeric materials C. Diffusion D. Large deformations E. Thermodynamics

1 Introduction

Elastomeric materials consist of a three-dimensional network of long polymer molecules which are laterally attached to one another at occasional points along their length; the attachment points are called *cross-links*. The basic physical elements of the network are the portions of molecules reaching from one cross-linkage to the next, and are called the *chains* in the network. The elastic reactive forces in such materials arise principally from the *decrease* in the configurational entropy of the chains as the material is stretched.

There are numerous elastomeric materials which can absorb large quantities of suitable fluids without the essential skeletal network structure of the elastomer being disrupted by the action of the fluid. Such a polymer network, together with the fluid molecules, forms a swollen aggregate called an elastomeric *gel*.[1] Elastomeric gels are ubiquitous; they are found in foods and medicines, and they find use in several important and diverse applications including valves for microfluidic devices, and tissue engineering. Indeed, many body parts in humans and other animals are gel-like in constitution.

Early studies of swelling of gels are due to Tanaka and co-workers (cf., e.g., Tanaka and Filmore, 1979), and in recent years there have been several notable attempts to formulate a coupled deformation-diffusion

---

*Tel.: +1-617-253-1635; E-mail address: anand@mit.edu

[1]Gels can also be made from colloidal solutions, and such gels are called *colloidal gels*. In this paper we restrict our attention to elastomeric gels, and within this class of materials we further restrict our attention to *non-ionic* gels.

theory for describing more complete aspects of the response of gels, including swelling and drying, squeezing of fluid by applied mechanical deformation, and forced permeation; cf., e.g., Durning and Morman (1993), Baek and Srinivasa (2004), Hong et al. (2008), Doi (2009), and the recent paper of Duda et al. (2010), and references to the vast literature therein. However, a suitable theory appears still not to be widely agreed upon. The purpose of this paper is to develop a thermodynamically-consistent, large-deformation, continuum-mechanical theory to describe the mutual interaction of mechanics and chemistry for solids capable of absorbing fluid-like chemical species, when the fluid-solid mixture is treated as *a single homogenized continuum body which allows for a mass flux of the fluid.*[2] Although differing in the details of its development, our theory has many similarities to the recent theories of Hong et al. (2008) and Duda et al. (2010).[3]

An essential kinematical ingredient of our theory is a multiplicative decomposition

$$\mathbf{F} = \mathbf{F}^e\mathbf{F}^s, \qquad \text{with} \qquad \mathbf{F}^s = \lambda^s\mathbf{1}, \qquad \lambda^s > 0,$$

of the deformation gradient $\mathbf{F}$ into elastic and swelling parts $\mathbf{F}^e$ and $\mathbf{F}^s$, respectively, with the swelling taken to be isotropic, where λ^s is the swelling stretch.[4] The roots of this kinematical decomposition of $\mathbf{F}$ for discussing the swelling and mechanical stretching of elastomeric materials are attributed to Flory (1950).[5] Following Flory (1950, 1953), Boyce and Arruda (2001), and Duda et al. (2010), we adopt this kinematical decomposition of $\mathbf{F}$ in formulating our coupled deformation-diffusion theory.

In what follows, we review the basic laws for the balance of forces and the balance of fluid content, and formulate a frame-indifferent and thermodynamically-consistent coupled deformation-diffusion theory for elastomeric gels. In discussing special constitutive equations, we limit our attention to isotropic materials, and consider a model for the free energy based on a Flory-Huggins theory for the free energy change due to mixing of the fluid with the polymer network (cf., e.g., Doi, 1996, 2009), and a statistical-mechanical model for the change in configurational entropy of the polymer chains as they are stretched. It has been common practice in the recent literature on the swelling of gels (Baek and Srinivasa, 2004; Hong et al., 2008; Doi, 2009; Duda et al., 2010) to model the changes in configurational entropy due to mechanical stretching, based on classical Gaussian-statistics, which unfortunately is valid only for small stretches. For larger stretches, as are typically encountered in highly-swollen gels, it is necessary to use non-Gaussian statistics to account for the limited extensibility of the polymer chains. Thus, unlike the recent theories in the literature, here we consider a mechanical contribution to the free energy based on the more realistic non-Gaussian statistics (cf., Treloar, 1975; Arruda and Boyce, 1993; Anand, 1996; Bischoff et al., 2001).

As representative examples of application of the theory, we study (a) isotropic three-dimensional swelling-equilibrium of an elastomeric gel in an unconstrained, stress-free state; and (b) the following one-dimensional transient problems: (i) free-swelling of a gel; (ii) consolidation of an already swollen gel; and (iii) pressure-difference-driven diffusion of organic solvents across elastomeric membranes. For the last example, we also compare results from our numerical calculations, against corresponding experimental results of Paul and Ebra-Lima (1970) for the steady-state diffusion across a membrane.

---

[2]And not as a multi-component mixture, as in the *Theory of Mixtures* (cf. e.g. Bowen, 1969; Truesdell, 1984; Rajagopal, 2003); as is well-known, there are inherent difficulties associated with specifying boundary conditions within the context of a mixture theory.

[3]However, we do note that while the basic balance laws are deduced by Duda et al. (2010) by adapting a virtual-power format proposed by Podio-Guidugli (2009), here we follow a different, more traditional and direct approach, which is in the spirit of the developments of Fried and Gurtin (1999, 2004) for coupled elastic deformation and diffusion of atomic/molecular species.

[4]Such a decomposition is widely used in plasticity theories, where $\mathbf{F}^s$ is written as $\mathbf{F}^p$, and represents the plastic part of $\mathbf{F}$ (Kröner, 1960; Lee 1969); in plasticity theory $\mathbf{F}^p$ is of course not taken to be spherical. Also see Lubarda (2004), who discusses the history and use of such a multiplicative decomposition of the deformation gradient in a variety of situations, including isotropic thermoelasticity, and isotropic growth in bio-mechanics.

[5]An explicit decomposition of the deformation gradient is not apparent in the paper by Flory (1950); although, writing α for the stretch, he does distinguish between a total stretch α, and a swelling stretch α_s.

2 Kinematics

Consider a fluid-free (dry) macroscopically-homogeneous elastomeric body. In what follows, the spatially-continuous fields that define our continuum theory represent averages meant to apply at length scales which are large compared to the length scales associated with the molecular network and its microscopic-scale free-volume. We identify such a macroscopically-homogeneous body B with the region of space it occupies in a fixed *reference configuration*, and denote by $\mathbf{X}$ an arbitrary material point of B. A *motion* of B is then a smooth one-to-one mapping $\mathbf{x} = \boldsymbol{\chi}(\mathbf{X}, t)$ with *deformation gradient*, *velocity*, and *velocity gradient* given by[6]

$$\mathbf{F} = \nabla \boldsymbol{\chi}, \qquad \mathbf{v} = \dot{\boldsymbol{\chi}}, \qquad \mathbf{L} = \operatorname{grad} \mathbf{v} = \dot{\mathbf{F}} \mathbf{F}^{-1}. \tag{2.1}$$

We base the theory on a multiplicative decomposition of the deformation gradient

$$\mathbf{F} = \mathbf{F}^e \mathbf{F}^s, \qquad \text{with} \qquad \mathbf{F}^s = \lambda^s \mathbf{1}, \qquad \lambda^s > 0. \tag{2.2}$$

Here, suppressing the argument t:

- $\mathbf{F}^s(\mathbf{X})$ represents the local distortion of the material at $\mathbf{X}$ due to swelling, and λ^s is the *swelling stretch*. This local deformation accounts for the swelling of the material due to absorbed fluid molecules which are pinned to the *coherent polymer network structure* that resides in the *structural space*[7] at $\mathbf{X}$ (as represented by the range of $\mathbf{F}^s(\mathbf{X})$);

- $\mathbf{F}^e(\mathbf{X})$ represents the subsequent stretching and rotation of this coherent swollen network structure, and thereby represents a corresponding mechanical elastic distortion.

We refer to $\mathbf{F}^s$ and $\mathbf{F}^e$ as the *swelling and elastic distortions*. Figure 1 schematically shows the mapping properties of $\mathbf{F}$, $\mathbf{F}^s$, and $\mathbf{F}^e$.

We write

$$J \overset{\text{def}}{=} \det \mathbf{F} > 0, \tag{2.3}$$

and hence, using (2.2),

$$J = J^e J^s, \qquad \text{where} \qquad J^e \overset{\text{def}}{=} \det \mathbf{F}^e > 0 \qquad \text{and} \qquad J^s \overset{\text{def}}{=} \det \mathbf{F}^s > 0. \tag{2.4}$$

Thus, using $(2.2)_2$,

$$J^s = (\lambda^s)^3. \tag{2.5}$$

As is standard,

$$\mathbf{F} = \mathbf{R}\mathbf{U} = \mathbf{V}\mathbf{R} \qquad \text{and} \qquad \mathbf{F}^e = \mathbf{R}^e \mathbf{U}^e = \mathbf{V}^e \mathbf{R}^e, \tag{2.6}$$

denote the right and left polar decompositions of $\mathbf{F}$ and $\mathbf{F}^e$, respectively, with $\mathbf{U}$, $\mathbf{V}$, $\mathbf{U}^e$ and $\mathbf{V}^e$ symmetric and positive definite tensors, and $\mathbf{R}$ and $\mathbf{R}^e$ rotations. Also, the tensors

$$\mathbf{C} = \mathbf{U}^2 = \mathbf{F}^\top \mathbf{F}, \quad \mathbf{B} = \mathbf{V}^2 = \mathbf{F}\mathbf{F}^\top, \quad \text{and} \quad \mathbf{C}^e = \mathbf{U}^{e2} = \mathbf{F}^{e\top} \mathbf{F}^e, \qquad \mathbf{B}^e = \mathbf{V}^{e2} = \mathbf{F}^e \mathbf{F}^{e\top}, \tag{2.7}$$

denote the total and elastic right and left Cauchy-Green tensors.

Next, by $(2.1)_3$ and (2.2),

$$\mathbf{L} = \mathbf{L}^e + \mathbf{F}^e \mathbf{L}^s \mathbf{F}^{e-1}, \tag{2.8}$$

with

$$\mathbf{L}^e = \dot{\mathbf{F}}^e \mathbf{F}^{e-1}, \qquad \mathbf{L}^s = \dot{\mathbf{F}}^s \mathbf{F}^{s-1}. \tag{2.9}$$

---

[6]Notation: We use standard notation of modern continuum mechanics (Gurtin et al., 2010). Specifically: ∇ and Div denote the gradient and divergence with respect to the material point $\mathbf{X}$ in the reference configuration; grad and div denote these operators with respect to the point $\mathbf{x} = \boldsymbol{\chi}(\mathbf{X}, t)$ in the deformed body; a superposed dot denotes the material time-derivative. Throughout, we write $\mathbf{F}^{e-1} = (\mathbf{F}^e)^{-1}$, $\mathbf{F}^{e-\top} = (\mathbf{F}^e)^{-\top}$, etc. We write $\operatorname{tr}\mathbf{A}$, $\operatorname{sym}\mathbf{A}$, $\operatorname{skw}\mathbf{A}$, $\mathbf{A}_0$, and $\operatorname{sym}_0\mathbf{A}$ respectively, for the trace, symmetric, skew, deviatoric, and symmetric-deviatoric parts of a tensor $\mathbf{A}$. Also, the inner product of tensors $\mathbf{A}$ and $\mathbf{B}$ is denoted by $\mathbf{A} : \mathbf{B}$, and the magnitude of $\mathbf{A}$ by $|\mathbf{A}| = \sqrt{\mathbf{A} : \mathbf{A}}$.

[7]Also sometimes referred to as the *intermediate* or *relaxed* local space at $\mathbf{X}$.

As is standard, we define the elastic and swelling stretching and spin tensors through

$$\left.\begin{aligned}
\mathbf{D}^e = \operatorname{sym}\mathbf{L}^e, \qquad \mathbf{W}^e = \operatorname{skw}\mathbf{L}^e, \\
\mathbf{D}^s = \operatorname{sym}\mathbf{L}^s, \qquad \mathbf{W}^s = \operatorname{skw}\mathbf{L}^s,
\end{aligned}\right\} \tag{2.10}$$

so that $\mathbf{L}^e = \mathbf{D}^e + \mathbf{W}^e$ and $\mathbf{L}^s = \mathbf{D}^s + \mathbf{W}^s$.

Further from (2.2), (2.9)$_2$, and (2.10)

$$\mathbf{D}^s = \left(\dot{\lambda}^s \lambda^{s-1}\right)\mathbf{1} \qquad \text{and} \qquad \mathbf{W}^s = \mathbf{0}; \tag{2.11}$$

and since

$$\dot{J}^s = J^s \operatorname{tr}\mathbf{D}^s, \tag{2.12}$$

we also have

$$\mathbf{D}^s = \frac{1}{3}\left(\dot{J}^s J^{s-1}\right)\mathbf{1}. \tag{2.13}$$

3 Frame-indifference

A *change in frame*, at each *fixed time* t is a transformation — defined by a rotation $\mathbf{Q}(t)$ and a spatial point $\mathbf{y}(t)$ — which transforms *spatial points* $\mathbf{x}$ to spatial points

$$\mathbf{x}^* = \mathcal{F}(\mathbf{x}), \tag{3.1}$$
$$= \mathbf{y}(t) + \mathbf{Q}(t)(\mathbf{x} - \mathbf{o}), \tag{3.2}$$

the function $\mathcal{F}$ represents a rigid mapping of the observed space into itself, with $\mathbf{o}$ a fixed spatial origin. By (3.2) the transformation law for the motion $\mathbf{x} = \boldsymbol{\chi}(\mathbf{X}, t)$ has the form

$$\boldsymbol{\chi}^*(\mathbf{X}, t) = \mathbf{y}(t) + \mathbf{Q}(t)(\boldsymbol{\chi}(\mathbf{X}, t) - \mathbf{o}). \tag{3.3}$$

Hence the deformation gradient $\mathbf{F}$ transforms according to

$$\mathbf{F}^* = \mathbf{Q}\mathbf{F}. \tag{3.4}$$

The reference configuration and the intermediate structural space are independent of the choice of such changes in frame; thus the fields

$$\mathbf{F}^s = \lambda^s \mathbf{1}, \quad J^s, \quad \text{and} \quad \mathbf{L}^s \equiv \mathbf{D}^s = \left(\dot{J}^s J^{s-1}\right)\mathbf{1} \quad \text{are invariant under a change in frame,} \tag{3.5}$$

which also of course follows from the fact that $\mathbf{F}^s$ is spherical. This observation, (2.2), and (3.4) yield the transformation law

$$\mathbf{F}^{e\,*} = \mathbf{Q}\mathbf{F}^e. \tag{3.6}$$

4 Balance of forces and moments

Throughout, we denote by P an arbitrary *part* (subregion) of the reference body B with $\mathbf{n}_{\mathrm{R}}$ the outward unit normal on the boundary ∂P of P.

Since time scales associated with fluid diffusion are usually considerably longer than those associated with wave propagation, we neglect all inertial effects. Then standard considerations of balance of forces and moments, when expressed referentially, give:

(a) There exists a stress tensor $\mathbf{T}_{\mathrm{R}}$, called the Piola stress, such that the surface traction on an element of the surface ∂P of P, is given by

$$\mathbf{s}(\mathbf{n}_{\mathrm{R}}) = \mathbf{T}_{\mathrm{R}}\mathbf{n}_{\mathrm{R}}. \tag{4.1}$$

4

(b) $\mathbf{T}_R$ satisfies the macroscopic force balance

$$\text{Div}\,\mathbf{T}_R + \mathbf{b}_R = \mathbf{0}, \tag{4.2}$$

where $\mathbf{b}_R$ is an external body force per unit reference volume, which, consistent with neglect of inertial effects, is taken to be time-idependent.

(c) $\mathbf{T}_R$ obeys the the symmetry condition

$$\mathbf{T}_R\mathbf{F}^\top = \mathbf{F}\mathbf{T}_R^\top, \tag{4.3}$$

which represents a balance of moments.

Further, under a change in frame $\mathbf{T}_R$ transforms as

$$\mathbf{T}_R^* = \mathbf{Q}\mathbf{T}_R. \tag{4.4}$$

Finally, as is standard, the Piola stress $\mathbf{T}_R$ is related to the standard symmetric Cauchy stress $\mathbf{T}$ in the deformed body by

$$\mathbf{T}_R = J\,\mathbf{T}\,\mathbf{F}^{-\top}, \tag{4.5}$$

so that

$$\mathbf{T} = J^{-1}\mathbf{T}_R\mathbf{F}^\top. \tag{4.6}$$

5   Fluid content. Balance law for the fluid content

Let

$$c_R(\mathbf{X}, t) \tag{5.1}$$

denote the *number of fluid molecules absorbed by the elastomer, reckoned per unit volume of the dry reference configuration*. We call c_R the *fluid content*.

Define a *fluid flux* $\mathbf{j}_R$, measured per unit area, per unit time, so that $-\int_{\partial P}\mathbf{j}_R \cdot \mathbf{n}_R\,da_R$ represents the number of fluid molecules entering P across ∂P, per unit time. In this case the *balance law for fluid content* takes the form

$$\overline{\int_P c_R\,dv_R} = -\int_{\partial P}\mathbf{j}_R \cdot \mathbf{n}_R\,da_R, \tag{5.2}$$

for every part P. Bringing the time derivative in (5.2) inside the integral and using the divergence theorem on the integral over ∂P, we find that

$$\int_P (\dot{c}_R + \text{Div}\,\mathbf{j}_R)\,dv_R = 0. \tag{5.3}$$

Since P is arbitrary, this leads to a (local) *balance law for fluid content*

$$\dot{c}_R = -\text{Div}\,\mathbf{j}_R. \tag{5.4}$$

6   Free energy imbalance

We consider a purely mechanical theory based on an energy imbalance that represents the first two laws of thermodynamics under *isothermal conditions*. This imbalance requires that *the temporal increase in free energy of any part be less than or equal to the power expended on that part plus the free energy carried into P by fluid transport*. Thus, letting ψ_R denote the *free energy* per unit reference volume, the second law takes the form

$$\overline{\int_P \psi_R\,dv_R} \leq \int_{\partial P}\underbrace{\mathbf{T}_R\mathbf{n}_R}_{\mathbf{s}(\mathbf{n}_R)}\cdot\dot{\boldsymbol{\chi}}\,da_R + \int_P \mathbf{b}_R \cdot \dot{\boldsymbol{\chi}}\,dv_R + \mathcal{T}(P), \tag{6.1}$$

5

for each part P, where the term $\mathcal{T}(\mathrm{P})$ represents the free energy flow due to fluid transport. We characterize this flow through a **chemical potential** μ; specifically, following Gurtin (1996) and Fried and Gurtin (1999, 2004), we assume that the fluid flux $\mathbf{j}_{\mathrm{R}}$ carries with it a flux of energy described by $\mu \mathbf{j}_{\mathrm{R}}$, so that

$$\mathcal{T}(\mathrm{P}) = - \int_{\partial \mathrm{P}} \mu \mathbf{j}_{\mathrm{R}} \cdot \mathbf{n}_{\mathrm{R}} \, da_{\mathrm{R}}. \tag{6.2}$$

Thus, using (6.2) in (6.1) we are led to

$$\overline{\int_{\mathrm{P}} \dot{\psi}_{\mathrm{R}} \, dv_{\mathrm{R}}} \leq \int_{\partial \mathrm{P}} \mathbf{T}_{\mathrm{R}} \mathbf{n}_{\mathrm{R}} \cdot \dot{\boldsymbol{\chi}} \, da_{\mathrm{R}} + \int_{\mathrm{P}} \mathbf{b}_{\mathrm{R}} \cdot \dot{\boldsymbol{\chi}} \, dv_{\mathrm{R}} - \int_{\partial \mathrm{P}} \mu \mathbf{j}_{\mathrm{R}} \cdot \mathbf{n}_{\mathrm{R}} \, da_{\mathrm{R}}. \tag{6.3}$$

Bringing the time derivative inside the integral, and using the divergence theorem on the integrals over $\partial \mathrm{P}$, reduces (6.3) to

$$\int_{\mathrm{P}} \dot{\psi}_{\mathrm{R}} \, dv_{\mathrm{R}} \leq \int_{\mathrm{P}} \left(\mathbf{T}_{\mathrm{R}} : \dot{\mathbf{F}} - \mu \mathrm{Div} \, \mathbf{j}_{\mathrm{R}} - \mathbf{j}_{\mathrm{R}} \cdot \nabla \mu \right) dv_{\mathrm{R}} + \int_{\mathrm{P}} \left(\mathrm{Div} \, \mathbf{T}_{\mathrm{R}} + \mathbf{b}_{\mathrm{R}} \right) \cdot \dot{\boldsymbol{\chi}} \, dv_{\mathrm{R}}. \tag{6.4}$$

Using (4.2) and (5.4), and since P is arbitrary, (6.4) yields the local free energy imbalance

$$\dot{\psi}_{\mathrm{R}} - \mathbf{T}_{\mathrm{R}} : \dot{\mathbf{F}} - \mu \dot{c}_{\mathrm{R}} + \mathbf{j}_{\mathrm{R}} \cdot \nabla \mu \leq 0. \tag{6.5}$$

Next, using (2.2) , $(2.9)_2$ and (4.5),

$$
\begin{aligned}
\mathbf{T}_{\mathrm{R}} : \dot{\mathbf{F}} &= \mathbf{T}_{\mathrm{R}} : (\dot{\mathbf{F}}^e \mathbf{F}^s + \mathbf{F}^e \dot{\mathbf{F}}^s) \\
&= (\mathbf{T}_{\mathrm{R}} \mathbf{F}^{s\top}) : \dot{\mathbf{F}}^e + (\mathbf{F}^{e\top} \mathbf{T}_{\mathrm{R}}) : \dot{\mathbf{F}}^s, \\
&= (\mathbf{T}_{\mathrm{R}} \mathbf{F}^{s\top}) : \dot{\mathbf{F}}^e + (\mathbf{F}^{e\top} \mathbf{T}_{\mathrm{R}} \mathbf{F}^{s\top}) : \mathbf{L}^s, \\
&= (J \mathbf{T} \mathbf{F}^{e-\top}) : \dot{\mathbf{F}}^e + (J \mathbf{F}^{e\top} \mathbf{T} \mathbf{F}^{e-\top}) : \mathbf{L}^s.
\end{aligned}
$$

For convenience, we define two new stress measures

$$\mathbf{T}^e \overset{\text{def}}{=} J \mathbf{T} \mathbf{F}^{e-\top} \qquad \text{and} \qquad \mathbf{M}^e \overset{\text{def}}{=} J \mathbf{F}^{e\top} \mathbf{T} \mathbf{F}^{e-\top}. \tag{6.6}$$

Then

$$\mathbf{T}_{\mathrm{R}} : \dot{\mathbf{F}} = \mathbf{T}^e : \dot{\mathbf{F}}^e + \mathbf{M}^e : \mathbf{L}^s. \tag{6.7}$$

Next, recalling $(2.11)_2$ and (2.13), we may write (6.7) as

$$\mathbf{T}_{\mathrm{R}} : \dot{\mathbf{F}} = \mathbf{T}^e : \dot{\mathbf{F}}^e + \frac{1}{3} J^{s-1} (\mathrm{tr} \, \mathbf{M}^e) \dot{J}^s. \tag{6.8}$$

Let

$$\bar{p} \overset{\text{def}}{=} -\frac{1}{3} J^{s-1} (\mathrm{tr} \, \mathbf{M}^e) = -\frac{1}{3} J^{s-1} \mathrm{tr} \left(J \mathbf{F}^{e\top} \mathbf{T} \mathbf{F}^{e-\top} \right) = -\frac{1}{3} J^e \mathrm{tr} \, \mathbf{T}, \tag{6.9}$$

define a mean normal pressure. Then, using (6.9), the stress-power (6.8) may be written as

$$\mathbf{T}_{\mathrm{R}} : \dot{\mathbf{F}} = \mathbf{T}^e : \dot{\mathbf{F}}^e - \bar{p} \dot{J}^s. \tag{6.10}$$

Hence, using (6.10) in (6.5), the local free energy imbalance may be written as

$$\dot{\psi}_{\mathrm{R}} - \mathbf{T}^e : \dot{\mathbf{F}}^e + \bar{p} \dot{J}^s - \mu \dot{c}_{\mathrm{R}} + \mathbf{j}_{\mathrm{R}} \cdot \nabla \mu \leq 0. \tag{6.11}$$

6

6.1 Kinematical constraint between c_{R} and J^s for elastomers

Now,

$$J^s - 1 \tag{6.12}$$

represents the change in volume per unit reference volume due to swelling. *We assume that this change arises entirely due to the change in the fluid content*, so that with v denoting the volume of a fluid molecule (presumed to be constant) we have the important *swelling constraint*

$$J^s = 1 + v c_{\mathrm{R}}, \tag{6.13}$$

or equivalently that

$$\dot{J}^s = v \dot{c}_{\mathrm{R}}. \tag{6.14}$$

Note that on account of (2.5), the constraint (6.14) may also be stated as

$$\lambda^s = (1 + v c_{\mathrm{R}})^{1/3}. \tag{6.15}$$

Upon enforcing the constraint (6.14), the free energy imbalance (6.11) becomes

$$\dot{\psi}_{\mathrm{R}} - \mathbf{T}^e : \dot{\mathbf{F}}^e - \mu_{\mathrm{act}}\, \dot{c}_{\mathrm{R}} + \mathbf{j}_{\mathrm{R}} \cdot \nabla \mu \leq 0, \tag{6.16}$$

where we have written

$$\mu_{\mathrm{act}} \overset{\mathrm{def}}{=} \mu - \bar{p}\, v\,, \tag{6.17}$$

for an *active* chemical potential.

6.2 Kinematical constraint of elastic incompressibility

As is standard, we consider the permeating fluid to be incompressible. Next, for most elastomeric materials the bulk modulus is two or more orders of magnitude higher than the shear modulus, and these materials are also typically approximated to be mechanically incompressible. Accordingly, we consider the overall mechanical or "elastic" response of an elastomeric gel to be *incompressible*. This assumption is embodied in the constraint

$$J^e \equiv \det \mathbf{F}^e = 1, \tag{6.18}$$

or equivalently that

$$\dot{J}^e = J^e \mathrm{tr}\,(\dot{\mathbf{F}}^e \mathbf{F}^{e-1}) = 0 \quad \Rightarrow \quad \mathrm{tr}\,(\dot{\mathbf{F}}^e \mathbf{F}^{e-1}) = 0 \quad \Rightarrow \quad \mathbf{F}^{e-\top} : \dot{\mathbf{F}}^e = 0. \tag{6.19}$$

The essential change induced by the constraint of elastic incompressibility lies with how the elastic stress power $\mathbf{T}^e : \dot{\mathbf{F}}^e$ enters the free energy imbalance (6.16). Note that the elastic stress power is unaltered by adding a term of the form $P\,\mathbf{F}^{e-\top} : \dot{\mathbf{F}}^e$, where P is an *arbitrary scalar field*. We may therefore write

$$\mathbf{T}^e : \dot{\mathbf{F}}^e = \mathbf{T}^e : \dot{\mathbf{F}}^e + \underbrace{P\,\mathbf{F}^{e-\top} : \dot{\mathbf{F}}^e}_{=0} = \mathbf{T}^e_{\mathrm{act}} : \dot{\mathbf{F}}^e, \tag{6.20}$$

where

$$\mathbf{T}^e_{\mathrm{act}} \overset{\mathrm{def}}{=} \mathbf{T}^e + P\,\mathbf{F}^{e-\top}, \tag{6.21}$$

defines an *active* elastic stress. Also, recalling $(6.6)_1$, $\mathbf{T}^e$ itself is now given by

$$\mathbf{T}^e = J^s \mathbf{T} \mathbf{F}^{e-\top}. \tag{6.22}$$

Thus, accounting for the elastic incompressibility constraint, the free energy imbalance (6.16) becomes

$$\dot{\psi}_{\mathrm{R}} - \mathbf{T}^e_{\mathrm{act}} : \dot{\mathbf{F}}^e - \mu_{\mathrm{act}}\, \dot{c}_{\mathrm{R}} + \mathbf{j}_{\mathrm{R}} \cdot \nabla \mu \leq 0. \tag{6.23}$$

In what follows we shall prescribe a constitutive equation for $\mathbf{T}^e_{\mathrm{act}}$. The field P does not expend power; it is irrelevant to the internal thermodynamic structure of the theory and for that reason is considered

indeterminate — that is, *it is not specified constitutively*; instead it is determined by the solution to the mechanical boundary value problem with appropriate boundary conditions.

Using (3.4) and (4.4), we note that $\mathbf{T}^e_{\mathrm{act}}$ transforms as

$$\mathbf{T}^{e*}_{\mathrm{act}} = \mathbf{Q}\mathbf{T}^e_{\mathrm{act}}, \tag{6.24}$$

under a change in frame, and also that

$$\psi_{\mathrm{R}}, \ \bar{p}, \ \mu \ \text{ and } \nabla\mu \text{ are invariant under a change in frame;} \tag{6.25}$$

$\psi_{\mathrm{R}}, \bar{p}$, and μ because they are scalars, and $\nabla\mu$ because ∇ is a referential gradient.

7 Constitutive theory

7.1 Basic constitutive equations

Guided by the dissipation inequality (6.23), we assume that the free energy, ψ_{R}, the active stress, $\mathbf{T}^e_{\mathrm{act}}$, the active chemical potential, μ_{act}, and the fluid flux, $\mathbf{j}_{\mathrm{R}}$, are given by

$$\left.\begin{aligned} \psi_{\mathrm{R}} &= \hat{\psi}_{\mathrm{R}}(\mathbf{F}^e, c_{\mathrm{R}}), \\ \mathbf{T}^e_{\mathrm{act}} &= \hat{\mathbf{T}}^e_{\mathrm{act}}(\mathbf{F}^e, c_{\mathrm{R}}), \\ \mu_{\mathrm{act}} &= \hat{\mu}_{\mathrm{act}}(\mathbf{F}^e, c_{\mathrm{R}}), \\ \mathbf{j}_{\mathrm{R}} &= \hat{\mathbf{j}}_{\mathrm{R}}(\mathbf{F}^e, c_{\mathrm{R}}, \nabla\mu); \end{aligned}\right\} \tag{7.1}$$

with $\mathbf{F}^e$ constrained to satisfy $\det \mathbf{F}^e = 1$. For simplicity, from the outset we have assumed that the constitutive equations for the free energy, active stress, and active chemical potential are independent of $\nabla\mu$, and depend only on the mechanical deformation gradient $\mathbf{F}^e$ and the fluid content c_{R}.

7.2 Consequences of the principle of material frame-indifference

The principle of material frame-indifference asserts that the constitutive equations (7.1) must be independent of the observer. Using the transformation rules (3.6), (6.24) and (6.25), we find that the constitutive equations must satisfy

$$\left.\begin{aligned} \psi_{\mathrm{R}} &= \hat{\psi}_{\mathrm{R}}(\mathbf{Q}\mathbf{F}^e, c_{\mathrm{R}}), \\ \mathbf{T}^e_{\mathrm{act}} &= \mathbf{Q}^{\top}\hat{\mathbf{T}}^e_{\mathrm{act}}(\mathbf{Q}\mathbf{F}^e, c_{\mathrm{R}}), \\ \mu_{\mathrm{act}} &= \hat{\mu}_{\mathrm{act}}(\mathbf{Q}\mathbf{F}^e, c_{\mathrm{R}}), \\ \mathbf{j}_{\mathrm{R}} &= \hat{\mathbf{j}}_{\mathrm{R}}(\mathbf{Q}\mathbf{F}^e, c_{\mathrm{R}}, \nabla\mu), \end{aligned}\right\} \tag{7.2}$$

for every rotation $\mathbf{Q}$ and all $\mathbf{F}^e$, c_{R}, and $\nabla\mu$ in the domain of the constitutive functions.

By the polar decomposition theorem, $\mathbf{F}^e = \mathbf{R}^e\mathbf{U}^e$, where $\mathbf{R}^e$ is a rotation, and $\mathbf{U}^e$ is symmetric and positive definite. Since (7.28) must hold for all rotations $\mathbf{Q}$, they must hold when $\mathbf{Q}$ takes the value $\mathbf{R}^{e\top}$, in which case we obtain

$$\left.\begin{aligned} \psi_{\mathrm{R}} &= \hat{\psi}_{\mathrm{R}}(\mathbf{U}^e, c_{\mathrm{R}}), \\ \mathbf{T}^e_{\mathrm{act}} &= \mathbf{R}^e\hat{\mathbf{T}}^e_{\mathrm{act}}(\mathbf{U}^e, c_{\mathrm{R}}), \\ \mu_{\mathrm{act}} &= \hat{\mu}_{\mathrm{act}}(\mathbf{U}^e, c_{\mathrm{R}}), \\ \mathbf{j}_{\mathrm{R}} &= \hat{\mathbf{j}}_{\mathrm{R}}(\mathbf{U}^e, c_{\mathrm{R}}, \nabla\mu). \end{aligned}\right\} \tag{7.3}$$

Recall $(2.7)_3$, viz.

$$\mathbf{C}^e = \mathbf{F}^{e\top}\mathbf{F}^e, \tag{7.4}$$

and in (7.28) replace $\mathbf{R}^e$ by $\mathbf{F}^e\mathbf{U}^{e-1}$ and $\mathbf{U}^e$ by $\sqrt{\mathbf{C}^e}$; this reduces (7.3) to

$$
\left.
\begin{aligned}
\psi_{\mathrm{R}} &= \bar{\psi}_{\mathrm{R}}(\mathbf{C}^e, c_{\mathrm{R}}), \\
\mathbf{T}^e_{\mathrm{act}} &= \mathbf{F}^e\bar{\mathbf{T}}^e_{\mathrm{act}}(\mathbf{C}^e, c_{\mathrm{R}}), \\
\mu_{\mathrm{act}} &= \bar{\mu}_{\mathrm{act}}(\mathbf{C}^e, c_{\mathrm{R}}), \\
\mathbf{j}_{\mathrm{R}} &= \bar{\mathbf{j}}_{\mathrm{R}}(\mathbf{C}^e, c_{\mathrm{R}}, \nabla\mu).
\end{aligned}
\right\}
\tag{7.5}
$$

7.3 Thermodynamic restrictions

With a view towards determining the restrictions imposed by the local free energy imbalance (6.23), note that

$$
\dot{\psi}_{\mathrm{R}} = \frac{\partial\bar{\psi}_{\mathrm{R}}}{\partial\mathbf{C}^e} : \dot{\mathbf{C}}^e + \frac{\partial\bar{\psi}_{\mathrm{R}}}{\partial c_{\mathrm{R}}}\,\dot{c}_{\mathrm{R}}.
\tag{7.6}
$$

Further, using the symmetry of $\partial\bar{\psi}_{\mathrm{R}}/\partial\mathbf{C}^e$,

$$
\frac{\partial\bar{\psi}_{\mathrm{R}}}{\partial\mathbf{C}^e} : \dot{\mathbf{C}}^e = \frac{\partial\bar{\psi}_{\mathrm{R}}}{\partial\mathbf{C}^e} : (2\mathbf{F}^{e\top}\dot{\mathbf{F}}^e) = \left(2\mathbf{F}^e\frac{\partial\bar{\psi}_{\mathrm{R}}}{\partial\mathbf{C}^e}\right) : \dot{\mathbf{F}}^e.
$$

Thus,

$$
\dot{\psi}_{\mathrm{R}} = \left(2\mathbf{F}^e\frac{\partial\bar{\psi}_{\mathrm{R}}}{\partial\mathbf{C}^e}\right) : \dot{\mathbf{F}}^e + \frac{\partial\bar{\psi}_{\mathrm{R}}}{\partial c_{\mathrm{R}}}\dot{c}_{\mathrm{R}}.
\tag{7.7}
$$

If we substitute (7.5) and (7.7) into (6.23) we find that

$$
\left(2\mathbf{F}^e\frac{\partial\bar{\psi}_{\mathrm{R}}}{\partial\mathbf{C}^e} - \mathbf{F}^e\bar{\mathbf{T}}^e_{\mathrm{act}}\right) : \dot{\mathbf{F}}^e + \left(\frac{\partial\bar{\psi}_{\mathrm{R}}}{\partial c_{\mathrm{R}}} - \bar{\mu}_{\mathrm{act}}\right)\dot{c}_{\mathrm{R}} + \bar{\mathbf{j}}_{\mathrm{R}}(\mathbf{C}^e, c_{\mathrm{R}}, \nabla\mu)\cdot\nabla\mu \le 0.
\tag{7.8}
$$

This inequality is to hold for all values of $\mathbf{C}^e$, c_{R}, and $\nabla\mu$. Since $\dot{\mathbf{F}}^e$ and $\dot{c}_{\mathrm{R}}$ appear linearly, their "coefficients" must vanish, for otherwise $\dot{\mathbf{F}}^e$ and $\dot{c}_{\mathrm{R}}$, may be chosen to violate (7.8). We are therefore led to the thermodynamic restrictions that the free energy determines the active stress $\mathbf{T}^e_{\mathrm{act}}$ and the active chemical potential μ_{act} through the "state relations"

$$
\left.
\begin{aligned}
\mathbf{T}^e_{\mathrm{act}} &= 2\mathbf{F}^e\frac{\partial\bar{\psi}_{\mathrm{R}}(\mathbf{C}^e, c_{\mathrm{R}})}{\partial\mathbf{C}^e}, \\
\mu_{\mathrm{act}} &= \frac{\partial\bar{\psi}_{\mathrm{R}}(\mathbf{C}^e, c_{\mathrm{R}})}{\partial c_{\mathrm{R}}},
\end{aligned}
\right\}
\tag{7.9}
$$

and that the response function $\bar{\mathbf{j}}_{\mathrm{R}}$ satisfies the *fluid-transport inequality*

$$
\bar{\mathbf{j}}_{\mathrm{R}}(\mathbf{C}^e, c_{\mathrm{R}}, \nabla\mu)\cdot\nabla\mu \le 0.
\tag{7.10}
$$

We assume henceforth that the fluid-transport inequality is *strict* in the sense that

$$
\bar{\mathbf{j}}_{\mathrm{R}}(\mathbf{C}^e, c_{\mathrm{R}}, \nabla\mu)\cdot\nabla\mu < 0 \qquad \text{when} \qquad \nabla\mu \ne \mathbf{0}.
\tag{7.11}
$$

Recalling (6.17) and (6.21), the state relations (7.9) yield

$$
\left.
\begin{aligned}
\mathbf{T}^e &= 2\mathbf{F}^e\frac{\partial\bar{\psi}_{\mathrm{R}}(\mathbf{C}^e, c_{\mathrm{R}})}{\partial\mathbf{C}^e} - P\mathbf{F}^{e-\top}, \\
\mu &= \frac{\partial\bar{\psi}_{\mathrm{R}}(\mathbf{C}^e, c_{\mathrm{R}})}{\partial c_{\mathrm{R}}} + \bar{p}v.
\end{aligned}
\right\}
\tag{7.12}
$$

Further, recalling that

$$
J^e = 1, \qquad J \equiv J^s = (1 + vc_{\mathrm{R}}), \qquad \mathbf{T}^e = J\mathbf{T}\mathbf{F}^{e-\top}, \qquad \text{and} \qquad \mathbf{T}_{\mathrm{R}} = \mathbf{T}^e\mathbf{F}^{s-\top},
\tag{7.13}
$$

9

(7.12) gives

$$\mathbf{T} = J^{-1} \left[2\mathbf{F}^e \frac{\partial \bar{\psi}_{\mathrm{R}}(\mathbf{C}^e, c_{\mathrm{R}})}{\partial \mathbf{C}^e} \mathbf{F}^{e\top} - P\mathbf{1} \right], \tag{7.14}$$

and

$$\mathbf{T}_{\mathrm{R}} = 2\mathbf{F}^e \frac{\partial \bar{\psi}_{\mathrm{R}}(\mathbf{C}^e, c_{\mathrm{R}})}{\partial \mathbf{C}^e} \mathbf{F}^{s-\top} - P\mathbf{F}^{-\top}. \tag{7.15}$$

Also, from (6.9) and (7.14),

$$\bar{p} = -\frac{1}{3} \left(J^{-1} 2\, \mathbf{C}^e : \frac{\partial \bar{\psi}_{\mathrm{R}}(\mathbf{C}^e, c_{\mathrm{R}})}{\partial \mathbf{C}^e} \right) + J^{-1} P. \tag{7.16}$$

For later use, we note that from $(7.12)_2$ and use of the chain-rule, that

$$\dot{\mu} - \dot{\bar{p}}\, v = \left(\frac{\partial^2 \bar{\psi}_{\mathrm{R}}(\mathbf{C}^e, c_{\mathrm{R}})}{\partial c_{\mathrm{R}} \partial \mathbf{C}^e} \right) : \dot{\mathbf{C}}^e + \left(\frac{\partial^2 \bar{\psi}_{\mathrm{R}}(\mathbf{C}^e, c_{\mathrm{R}})}{\partial c_{\mathrm{R}}^2} \right) \dot{c}_{\mathrm{R}}. \tag{7.17}$$

For convenience, we introduce a scalar modulus $\Lambda(\mathbf{C}^e, c_{\mathrm{R}})$, and a tensor modulus $\mathbf{\Lambda}(\mathbf{C}^e, c_{\mathrm{R}})$, defined by

$$\Lambda(\mathbf{C}^e, c_{\mathrm{R}}) \stackrel{\text{def}}{=} \left(\frac{\partial^2 \bar{\psi}_{\mathrm{R}}(\mathbf{C}^e, c_{\mathrm{R}})}{\partial c_{\mathrm{R}}^2} \right) \quad \text{and} \quad \mathbf{\Lambda}(\mathbf{C}^e, c_{\mathrm{R}}) \stackrel{\text{def}}{=} \left(\frac{\partial^2 \bar{\psi}_{\mathrm{R}}(\mathbf{C}^e, c_{\mathrm{R}})}{\partial c_{\mathrm{R}} \partial \mathbf{C}^e} \right). \tag{7.18}$$

We assume further that the scalar modulus $\Lambda(\mathbf{C}^e, c_{\mathrm{R}})$ is *non-zero*, so that by (7.17), $\dot{c}_{\mathrm{R}}$ may be related to changes in μ, $\bar{p}$ and $\mathbf{C}^e$ by

$$\dot{c}_{\mathrm{R}} = \Lambda(\mathbf{C}^e, c_{\mathrm{R}})^{-1} \left(\dot{\mu} - \dot{\bar{p}}\, v - \mathbf{\Lambda}(\mathbf{C}^e, c_{\mathrm{R}}) : \dot{\mathbf{C}}^e \right). \tag{7.19}$$

7.4 Fluid flux

We assume henceforth that the constitutive equation $(7.5)_4$ for the fluid flux obeys a Darcy-type relation. That is, the fluid flux $\mathbf{j}_{\mathrm{R}}$ depends *linearly* on the chemical potential gradient $\nabla\mu$,

$$\mathbf{j}_{\mathrm{R}} = -\mathbf{M}(\mathbf{C}^e, c_{\mathrm{R}}) \nabla\mu, \tag{7.20}$$

where $\mathbf{M}$ is a mobility tensor. Note that on account of (7.11), the mobility tensor is positive definite.

Remark 1:
The general equations derived in this paper have been recently also derived (from different beginnings and in a different notation) by Duda et al. (2010). The following correspondence exists between the work of Duda et al., and that presented here:

1. Balance of forces and fluid content: Duda et al. eq. (8) $\equiv$ Eqs. (4.2) and (5.4) of this paper.

2. Free energy imbalance: Duda et al. eq. (12) $\equiv$ Eq. (6.5).

3. State relations for stress and chemical potential: Duda et al. eq. (28) $\equiv$ Eq. (7.12).

4. Fluid-transport inequality: Duda et al. eq. (29) $\equiv$ Eq. (7.10).

7.5 Isotropic materials

Henceforth we confine our attention to *isotropic materials*. The following definitions help make precise our notion of an isotropic material (cf., Anand and Gurtin, 2003, and Anand et al., 2009):

(i) $\mathrm{Orth}^+ =$ the group of all rotations (the proper orthogonal group);

(ii) the *symmetry group* $\mathcal{G}_{\mathrm{R}}$, is the group of all rotations of the *reference* configuration that leaves the response of the material unaltered;

(iii) the *symmetry group* $\mathcal{G}_{\mathrm{I}}$ at each time t, is the group of all rotations of the *intermediate* structural space that leaves the response of the material unaltered.

We now discuss the manner in which the basic fields transform under such transformations.

7.5.1 Isotropy of the reference configuration

Let $\mathbf{Q}$ be a *time-independent rotation of the reference configuration*. Then $\mathbf{F} \to \mathbf{F}\mathbf{Q}$, and hence

$$\mathbf{F}^s \to \mathbf{F}^s\mathbf{Q}, \quad \text{and} \quad \mathbf{F}^e \text{ is invariant.} \tag{7.21}$$

We may therefore use $(2.7)_3$ to conclude that

$$\mathbf{C}^e \text{ is invariant.} \tag{7.22}$$

Since $\mathbf{T}^e_{\text{act}}$ and μ are derived from the free energy function, we need only focus on the effect of such a symmetry transformation of the reference space on $\bar{\psi}_{\text{R}}(\mathbf{C}^e, c_{\text{R}})$.

- Thus, using (7.22) we see that $\bar{\psi}_{\text{R}}(\mathbf{C}^e, c_{\text{R}})$ and hence the constitutive equations (7.12) are unaffected by such rotations of the reference configuration.

Next, concerning the constitutive equation (7.20) for the species flux, mimicking a standard result from the theory of finite thermoelasticity (cf., Gurtin, Fried, Anand, 2010, Section 57.8), under a symmetry transformation $\mathbf{Q}$ for the reference configuration, the referential gradient of the chemical potential $\nabla\mu$ and the species flux $\mathbf{j}_{\text{R}}$ transform as

$$\nabla\mu \to \mathbf{Q}^\top\nabla\mu, \qquad \mathbf{j}_{\text{R}} \to \mathbf{Q}^\top\mathbf{j}_{\text{R}}.$$

Hence, from (7.20) the mobility tensor must obey

$$\mathbf{M}(\mathbf{C}^e, c_{\text{R}}) = \mathbf{Q}^\top\mathbf{M}(\mathbf{C}^e, c_{\text{R}})\mathbf{Q} \tag{7.23}$$

for all rotations $\mathbf{Q}$ in the symmetry group $\mathcal{G}_{\text{R}}$.

We refer to the material as *initially isotropic* (and to the reference configuration as undistorted) if

$$\mathcal{G}_{\text{R}} = \text{Orth}^+ \tag{7.24}$$

so that the response of the material is invariant under arbitrary rotations of the reference space. Henceforth

- *we restrict attention to materials that are initially isotropic.*

In this case, the mobility tensor has the standard representation

$$\mathbf{M}(\mathbf{C}^e, c_{\text{R}}) = m(\mathbf{C}^e, c_{\text{R}})\mathbf{1}, \qquad \text{with} \qquad m(\mathbf{C}^e, c_{\text{R}}) > 0 \tag{7.25}$$

a scalar mobility.

7.5.2 Isotropy of the intermediate structural space

Next, let $\mathbf{Q}$, a *time-independent rotation of the intermediate space*, be a symmetry transformation. Then $\mathbf{F}$ is unaltered by such a rotation, and hence

$$\mathbf{F}^e \to \mathbf{F}^e\mathbf{Q} \quad \text{and} \quad \mathbf{F}^s \to \mathbf{Q}^\top\mathbf{F}^s, \tag{7.26}$$

and also

$$\mathbf{C}^e \to \mathbf{Q}^\top\mathbf{C}^e\mathbf{Q}. \tag{7.27}$$

Again, since $\mathbf{T}^e_{\text{act}}$ and μ are derived from the free energy function, we need only focus on the effect of such a symmetry transformation of the intermediate space on $\bar{\psi}_{\text{R}}(\mathbf{C}^e, c_{\text{R}})$. In addition we also need to consider the effect of the symmetry transformation on the scalar mobility $m(\mathbf{C}^e, c_{\text{R}})$ in (7.25). Using $(7.27)_1$ we conclude that

$$\left.\begin{array}{l} \bar{\psi}_{\text{R}}(\mathbf{C}^e, c_{\text{R}}) = \bar{\psi}_{\text{R}}(\mathbf{Q}^\top\mathbf{C}^e\mathbf{Q}, c_{\text{R}}), \\ m(\mathbf{C}^e, c_{\text{R}}) = m(\mathbf{Q}^\top\mathbf{C}^e\mathbf{Q}, c_{\text{R}}), \end{array}\right\} \tag{7.28}$$

must hold for all rotations $\mathbf{Q}$ in the *symmetry group* $\mathcal{G}_{\text{I}}$ at each time t.

We refer to the material as one which is *continually isotropic*, if in addition to the referential isotropy discussed in the previous subsection,

$$\mathcal{G}_{\text{I}} = \text{Orth}^+, \tag{7.29}$$

so that the response of the material is also invariant under arbitrary rotations of the intermediate space at each time t. Henceforth

- *we restrict attention to materials that are not only initially, but also continually isotropic.*

In this case, the response functions $\bar{\psi}_{\mathrm{R}}$ and m must also each be *isotropic*. Thus, $\bar{\psi}(\mathbf{C}^e, c_{\mathrm{R}})$ has the representation

$$\bar{\psi}(\mathbf{C}^e, c_{\mathrm{R}}) = \tilde{\psi}(\mathcal{I}_{\mathbf{C}^e}, c_{\mathrm{R}}), \tag{7.30}$$

where

$$\mathcal{I}_{\mathbf{C}^e} = \big(I_1(\mathbf{C}^e), I_2(\mathbf{C}^e)\big)$$

is the list of principal invariants of $\mathbf{C}^e$ for an elastically-incompressible material. Also the scalar mobility $m(\mathbf{C}^e, c_{\mathrm{R}})$ has the representation

$$m(\mathbf{C}^e, c_{\mathrm{R}}) = m(\mathcal{I}_{\mathbf{C}^e}, c_{\mathrm{R}}). \tag{7.31}$$

In this case (7.20) becomes[8]

$$\mathbf{j}_{\mathrm{R}} = -m(\mathcal{I}_{\mathbf{C}^e}, c_{\mathrm{R}}) \nabla \mu. \tag{7.32}$$

8 Specialization of the free energy function ψ_{R}

The constitutive equations considered thus far are fairly general. With a view towards applications we now specialize the theory by imposing additional constitutive assumptions. We begin by assuming that the free energy ψ_{R} may be written in a separable form as (cf., e.g., Flory, 1953)

$$\bar{\psi}_{\mathrm{R}}(\mathbf{C}^e, c_{\mathrm{R}}) = \mu^0 c_{\mathrm{R}} + \psi_{\mathrm{R,mixing}}(c_{\mathrm{R}}) + \psi_{\mathrm{R,mechanical}}(\mathbf{C}^e, c_{\mathrm{R}}), \tag{8.1}$$

where μ^0 is the chemical potential of the unmixed pure solvent, $\psi_{\mathrm{R,mixing}}(c_{\mathrm{R}})$ is the change in free energy due to mixing of the solvent with the polymer network, and $\psi_{\mathrm{R,mechanical}}(\mathbf{C}^e, c_{\mathrm{R}})$ is the contribution to the change in the free energy due to the deformation of the polymer network.

Estimate for $\psi_{\mathrm{R,mixing}}$

In the literature on swelling of elastomers, the quantity

$$\phi \stackrel{\mathrm{def}}{=} (1 + \upsilon c_{\mathrm{R}})^{-1} = (\lambda^s)^{-3} = J^{s-1}, \qquad 0 < \phi \leq 1, \tag{8.2}$$

is called the *polymer volume fraction*. The dry state corresponds to $\phi = 1$, and $\phi < 1$ represents a swollen state.

Following Doi (1996, 2009), we adopt the following form of the Flory (1942)-Huggins (1942) theory for the contribution to the free energy due to mixing

$$\psi_{\mathrm{R,mixing}} = \frac{k_B \vartheta}{\upsilon} \frac{1}{\phi} \Big((1 - \phi) \ln(1 - \phi) + \chi \phi (1 - \phi) \Big), \tag{8.3}$$

where k_B is Boltzmann's constant, ϑ is the absolute temperature, and χ is a dimensionless parameter (called the chi-parameter, or interaction parameter), which represents the dis-affinity between the polymer and the the fluid;

- if χ is increased the fluid molecules are expelled from the gel and the gel shrinks, while if χ is decreased, the gel swells.

The expression (8.3) for the mixing energy when expressed in terms of c_{R} is

$$\psi_{\mathrm{R,mixing}}(c_{\mathrm{R}}) = k_B \vartheta c_{\mathrm{R}} \left(\ln \left(\frac{\upsilon c_{\mathrm{R}}}{1 + \upsilon c_{\mathrm{R}}} \right) + \chi \left(\frac{1}{1 + \upsilon c_{\mathrm{R}}} \right) \right). \tag{8.4}$$

---

[8]Note that our eq. (7.32) for the referential fluid flux differs from eq. (67) of Duda et al. (2010), who presume an equation of the form $\mathbf{j} = -\hat{m}(c)\mathrm{grad}\,\mu$ in the deformed body (cf., also Section 4 of Hong et al., 2008). In our theory, material symmetry considerations involving rotations of the referential and structural space directly lead to (7.32).

Estimate for $\psi_{\mathrm{R,mechanical}}$

In elastomeric materials, the major part of $\psi_{\mathrm{R,mechanical}}$ arises from an "entropic" contribution. Let

$$\bar{\lambda} \stackrel{\text{def}}{=} \frac{1}{\sqrt{3}}\sqrt{\operatorname{tr}\mathbf{C}} \tag{8.5}$$

define an *effective stretch*, then classical statistical mechanics models of rubber elasticity (cf., Treloar, 1975; Arruda and Boyce, 1993; Anand, 1996; Bischoff et al., 2001) provide the following estimates for the entropy change due to mechanical stretching:

1. For small to moderate values of $\bar{\lambda}$, based on Gaussian statistics,

$$\eta_{\mathrm{R,mechanical}} = -\frac{3}{2}\,N_{\mathrm{R}}\,k_B\,(\bar{\lambda}^2 - 1) + N_{\mathrm{R}}\,k_B\ln J, \tag{8.6}$$

   where N_{R} represents the number of polymer chains per unit reference volume.

2. For larger values of $\bar{\lambda}$ it is necessary to use non-Gaussian statistics to account for the limited extensibility of the polymer chains, and for these circumstances the entropy change is given by

$$\eta_{\mathrm{R,mechanical}} = -N_{\mathrm{R}}k_B\lambda_L^2\left[\left(\frac{\bar{\lambda}}{\lambda_L}\right)\beta + \ln\left(\frac{\beta}{\sinh\beta}\right) - \left(\frac{1}{\lambda_L}\right)\beta_0 - \ln\left(\frac{\beta_0}{\sinh\beta_0}\right)\right] + N_{\mathrm{R}}k_B\ln J, \tag{8.7}$$

   with

$$\beta \stackrel{\text{def}}{=} \mathcal{L}^{-1}\left(\frac{\bar{\lambda}}{\lambda_L}\right), \qquad \text{and} \qquad \beta_0 \stackrel{\text{def}}{=} \mathcal{L}^{-1}\left(\frac{1}{\lambda_L}\right), \tag{8.8}$$

   where $\mathcal{L}^{-1}$ is the inverse of the Langevin function $\mathcal{L}(x) = \coth(x) - (x)^{-1}$. This functional form for the change in entropy involves two material parameters: N_{R}, the number of polymer chains per unit reference volume, and λ_L, the *network locking stretch*.[9]

In what follows, we consider the more general form (8.7) for the entropy change, but when needed we also specialize our results for the simpler estimate (8.6) based on Gaussian statistics.

Let ϑ denote the constant temperature under consideration. Then, neglecting any energetic contribution to mechanical stretching (as is typically assumed), using (2.4), (8.6) – (8.8), $J^e = 1$, the identities

$$\operatorname{tr}\mathbf{C} = (\lambda^s)^2\operatorname{tr}(\mathbf{C}^e) = (1 + \upsilon c_{\mathrm{R}})^{2/3}\operatorname{tr}(\mathbf{C}^e), \qquad \ln J = \ln(1 + \upsilon c_{\mathrm{R}}), \tag{8.9}$$

and writing

$$G_0 \stackrel{\text{def}}{=} N_{\mathrm{R}}\,k_{\mathrm{B}}\,\vartheta, \tag{8.10}$$

for a *ground-state shear modulus* at the constant temperature under consideration, we obtain the estimate

$$\psi_{\mathrm{R,mechanical}}(\mathbf{C}^e, c_{\mathrm{R}}) = G_0\lambda_L^2\left[\left(\frac{\bar{\lambda}}{\lambda_L}\right)\beta + \ln\left(\frac{\beta}{\sinh\beta}\right) - \left(\frac{1}{\lambda_L}\right)\beta_0 - \ln\left(\frac{\beta_0}{\sinh\beta_0}\right)\right] - G_0\ln(1 + \upsilon c_{\mathrm{R}}), \tag{8.11}$$

with

$$\beta = \mathcal{L}^{-1}\left(\frac{\bar{\lambda}}{\lambda_L}\right), \qquad \text{and} \qquad \beta_0 = \mathcal{L}^{-1}\left(\frac{1}{\lambda_L}\right), \tag{8.12}$$

where, using (8.5) and (8.9),

$$\bar{\lambda} = \hat{\bar{\lambda}}(\mathbf{C}^e, c_{\mathrm{R}}) = \frac{1}{\sqrt{3}}(1 + \upsilon c_{\mathrm{R}})^{1/3}\sqrt{\operatorname{tr}\mathbf{C}^e}. \tag{8.13}$$

---

[9]In the non-Gaussian model, the network locking stretch λ_L is related to the number of links n in a freely-jointed chain by $\lambda_L = \sqrt{n}$.

Total free energy, stress, chemical potential

Thus, using (8.4) and (8.11) in (8.1), a simple form of the free energy function which accounts for the combined effects of mixing, swelling, and elastic stretching is

$$
\begin{aligned}
\psi_{\mathrm{R}} = {}& \mu^0 c_{\mathrm{R}} + k_B \vartheta c_{\mathrm{R}} \left(\ln\left(\frac{v c_{\mathrm{R}}}{1 + v c_{\mathrm{R}}}\right) + \chi\left(\frac{1}{1 + v c_{\mathrm{R}}}\right) \right) \\
& + G_0 \lambda_L^2 \left[\left(\frac{\bar{\lambda}}{\lambda_L}\right)\beta + \ln\left(\frac{\beta}{\sinh\beta}\right) - \left(\frac{1}{\lambda_L}\right)\beta_0 - \ln\left(\frac{\beta_0}{\sinh\beta_0}\right) \right] - G_0 \ln(1 + v c_{\mathrm{R}}).
\end{aligned}
\tag{8.14}
$$

Then, using (7.14), we find that the Cauchy stress tensor is given by

$$
\mathbf{T} = J^{-1} \left[G\,(1 + v c_{\mathrm{R}})^{2/3} \mathbf{B}^e - P\mathbf{1} \right],
\tag{8.15}
$$

where

$$
G \stackrel{\text{def}}{=} G_0\,\zeta \qquad \text{with} \qquad \zeta \stackrel{\text{def}}{=} \left(\frac{\lambda_L}{3\bar{\lambda}}\right) \mathcal{L}^{-1}\left(\frac{\bar{\lambda}}{\lambda_L}\right),
\tag{8.16}
$$

is a *generalized shear modulus*, and $\mathbf{B}^e$ is the elastic left Cauchy-Green tensor. Note that since $\mathcal{L}^{-1}(z) \to \infty$ as $z \to 1$, the stretch-dependent shear modulus $G \to \infty$ as $(\bar{\lambda}/\lambda_L) \to 1$. Also, since the first two terms in the series expansion of the inverse Langevin function are $\mathcal{L}^{-1}(z) = 3\,z + (9/5)\,z^3 + \ldots$, for small departures of the effective stretch form unity we have $\zeta \approx 1$, and hence that $G \approx G_0$.

Next, on account of (2.5) and (6.14),

$$
(1 + v c_{\mathrm{R}})^{2/3} = (\lambda^s)^2,
$$

and also since

$$
\mathbf{B} = (\lambda^s)^2 \mathbf{B}^e,
\tag{8.17}
$$

where $\mathbf{B} = \mathbf{F}\mathbf{F}^\top$ is the left Cauchy-Green tensor, (8.15) reduces to

$$
\mathbf{T} = J^{-1} \left[G\,\mathbf{B} - P\mathbf{1} \right].
\tag{8.18}
$$

Hence the Piola stress, $\mathbf{T}_{\mathrm{R}} = J\mathbf{T}\mathbf{F}^{-\top}$, is given by

$$
\mathbf{T}_{\mathrm{R}} = G\mathbf{F} - P\mathbf{F}^{-\top}.
\tag{8.19}
$$

Also using (7.12)$_2$ and (8.14) the chemical potential μ is given by

$$
\begin{aligned}
\mu = {}& \mu^0 + k_B\vartheta\left(\ln\left(\frac{v c_{\mathrm{R}}}{1 + v c_{\mathrm{R}}}\right) + \frac{1}{(1 + v c_{\mathrm{R}})} + \chi\frac{1}{(1 + v c_{\mathrm{R}})^2} \right) \\
& + G\,\bar{\lambda}^2\,(1 + v c_{\mathrm{R}})^{-1}\,v - G_0\,(1 + v c_{\mathrm{R}})^{-1}\,v + \bar{p}v.
\end{aligned}
\tag{8.20}
$$

Further, from (6.9), (8.18), (8.13) and using (8.2), viz.

$$
J^{-1} \equiv J^{s-1} = (1 + v c_{\mathrm{R}})^{-1} = \phi,
$$

we obtain

$$\bar{p} = -J^{s-1} \left[G \frac{1}{3}(1 + vc_{\mathrm{R}})^{2/3} \mathrm{tr} \, \mathbf{B}^e - P \right],$$

$$= -G\bar{\lambda}^2(1 + vc_{\mathrm{R}})^{-1} + P\phi, \tag{8.21}$$

use of which in (8.20) gives

$$\mu = \mu^0 + k_B \vartheta \Big(\ln(1 - \phi) + \phi + \chi\phi^2 \Big) - vG_0\phi + vP\phi. \tag{8.22}$$

Remark 2:
For a theory based on Gaussian statistics for configurational changes in entropy, cf. eq. (8.6), the generalized shear modulus is no longer stretch-dependent, so that $G = G_0$, and the expression (8.18) for the stress, reduces to

$$\mathbf{T} = J^{-1}(G_0\mathbf{B} - P\mathbf{1}), \tag{8.23}$$

while the expression (8.22) for the chemical potential remains unchanged. In Section 10 where we discuss a few applications of our theory, we will compare results using a theory based on Gaussian statistics against those based on the more general non-Gaussian statistics.

9 Governing partial differential equations for the deformation and fluid content fields. Boundary conditions

The governing partial differential equations consist of

1. The swelling constraint (6.13) (with $\det \mathbf{F}^e = 1$),

$$\det \mathbf{F} = (1 + vc_{\mathrm{R}}). \tag{9.1}$$

2. The local force balance for the macroscopic Piola stress,

$$\mathrm{Div} \, \mathbf{T}_{\mathrm{R}} + \mathbf{b}_{\mathrm{R}} = \mathbf{0}, \tag{9.2}$$

with $\mathbf{T}_{\mathrm{R}}$ given by (8.19).

3. Use of (7.32) in the balance equation (5.4) for the fluid content gives

$$\dot{c}_{\mathrm{R}} = \mathrm{Div} \, (m\nabla\mu), \tag{9.3}$$

in which $m = \hat{m}(\mathcal{I}_{\mathbf{C}^e}, c_{\mathrm{R}}) > 0$ is the scalar fluid mobility, and the chemical potential μ is given by (8.22).

In applications it may be advantageous to use (7.19), (7.32), (8.13), and (8.20) and express (9.3) as

$$\dot{\mu} = \Lambda \, \mathrm{Div} \, (m\nabla\mu) + \dot{p}v + \mathbf{\Lambda} : \dot{\mathbf{C}}^e, \tag{9.4}$$

with the moduli

$$\Lambda \overset{\text{def}}{=} \frac{\partial^2 \bar{\psi}_{\mathrm{R}}(\mathbf{C}^e, c_{\mathrm{R}})}{\partial c_{\mathrm{R}}^2}$$

$$= k_B \vartheta \left[\frac{1}{c_{\mathrm{R}}(1 + vc_{\mathrm{R}})} - \frac{v}{(1 + vc_{\mathrm{R}})^2} - \frac{2\chi v}{(1 + vc_{\mathrm{R}})^3} \right] \tag{9.5}$$

$$- \frac{1}{3} G_0 \left[\zeta \, \bar{\lambda}^2 - \bar{\lambda}^3 \frac{\partial \zeta}{\partial \bar{\lambda}} \right] \frac{v^2}{(1 + vc_{\mathrm{R}})^2} + G_0 \frac{v}{(1 + vc_{\mathrm{R}})^2}, \tag{9.6}$$

and

$$\mathbf{\Lambda} \stackrel{\text{def}}{=} \frac{\partial^2 \bar{\psi}_{\mathrm{R}}(\mathbf{C}^e, c_{\mathrm{R}})}{\partial c_{\mathrm{R}} \partial \mathbf{C}^e} = \frac{1}{6} G_0 \left(\frac{\upsilon}{(1 + \upsilon c_{\mathrm{R}})^{1/3}} \right) \left(\bar{\lambda} \frac{\partial \zeta}{\partial \bar{\lambda}} + \frac{1}{2} \zeta \right) \mathbf{1}, \tag{9.7}$$

calculated from the free energy function (8.14).

We also need initial and boundary conditions to complete the model. Let $\mathcal{S}_{\boldsymbol{\chi}}$ and $\mathcal{S}_{\mathbf{t}}$ be *complementary subsurfaces* of the boundary $\partial \mathrm{B}$ of the body B in the sense $\partial \mathrm{B} = \mathcal{S}_{\boldsymbol{\chi}} \cup \mathcal{S}_{\mathbf{t}}$ and $\mathcal{S}_{\boldsymbol{\chi}} \cap \mathcal{S}_{\mathbf{t}} = \emptyset$. Similarly let $\mathcal{S}_{\mu}$ and $\mathcal{S}_{\mathbf{j}}$ be *complementary subsurfaces* of the boundary: $\partial \mathrm{B} = \mathcal{S}_{\mu} \cup \mathcal{S}_{\mathbf{j}}$ and $\mathcal{S}_{\mu} \cap \mathcal{S}_{\mathbf{j}} = \emptyset$. Then for a time interval $t \in [0, T]$ we consider a pair of boundary conditions in which the motion is specified on $\mathcal{S}_1$ and the surface traction on $\mathcal{S}_2$:

$$\left. \begin{aligned} \boldsymbol{\chi} &= \hat{\boldsymbol{\chi}} \quad \text{on } \mathcal{S}_{\boldsymbol{\chi}} \times [0, T], \\ \mathbf{T}_{\mathrm{R}} \mathbf{n}_{\mathrm{R}} &= \hat{\mathbf{t}}_{\mathrm{R}} \quad \text{on } \mathcal{S}_{\mathbf{t}} \times [0, T], \end{aligned} \right\} \tag{9.8}$$

and another pair of boundary conditions in which the chemical potential is specified on $\mathcal{S}_{\mu}$ and the fluid flux on $\mathcal{S}_{\mathbf{j}}$

$$\left. \begin{aligned} \mu &= \hat{\mu} \quad \text{on } \mathcal{S}_{\mu} \times [0, T], \\ -m(\nabla \mu) \cdot \mathbf{n}_{\mathrm{R}} &= \hat{j} \quad \text{on } \mathcal{S}_{\mathbf{j}} \times [0, T], \end{aligned} \right\} \tag{9.9}$$

with $\hat{\boldsymbol{\chi}}$, $\hat{\mathbf{t}}_{\mathrm{R}}$, $\hat{\mu}$, and $\hat{j}$ *prescribed* functions of $\mathbf{X}$ and t, and the initial data

$$\boldsymbol{\chi}(\mathbf{X}, 0) = \boldsymbol{\chi}_0(\mathbf{X}) \qquad \text{and} \qquad \mu(\mathbf{X}, 0) = \mu_0(\mathbf{X}) \qquad \text{in} \qquad \mathrm{B}. \tag{9.10}$$

The coupled set of equations (9.1), (9.2), and (9.4), together with (9.8), (9.9) and (9.10) yield an initial boundary-value problem for the motion $\boldsymbol{\chi}(\mathbf{X}, t)$ and the chemical potential $\mu(\mathbf{X}, t)$.

In applications, for the case in which the environment consists of a pure and incompressible liquid, the boundary condition on chemical potential $\hat{\mu}$ is given by

$$\hat{\mu} = \mu^0 + p_a \upsilon, \tag{9.11}$$

where μ^0 is a reference chemical potential, p_a is the hydrostatic pressure of the liquid (expressed referentially), and υ is the volume of a liquid molecule. Also, if a portion of the boundary is impermeable to the liquid, then on that portion the prescribed flux $\hat{j}$ vanishes.

10   Applications

In this section, as representative examples of application of the theory, we study (a) isotropic three-dimensional swelling-equilibrium of an elastomeric gel in an unconstrained, stress-free state; and (b) the following one-dimensional transient problems: (i) free-swelling of a gel; (ii) consolidation of an already swollen gel; and (iii) pressure-difference-driven diffusion of organic solvents across elastomeric membranes. For the last example, we also compare results from our numerical calculations, against corresponding experimental results of Paul and Ebra-Lima (1970) for the steady-state diffusion across a membrane.

We begin by specializing the mobility m. Referring to (7.31) we recall that the mobility for an isotropic material is in general a function of the invariants of the elastic Cauchy-Green tensor $\mathbf{C}^e$ and the fluid content c_{R},

$$m = \hat{m}(\mathcal{I}_{\mathbf{C}^e}, c_{\mathrm{R}}).$$

Not much is experimentally known about the dependence of m on $\mathcal{I}_{\mathbf{C}^e}$, and since the dominant dependence of the mobility is expected to result from the amount of swelling J^s, or equivalently c_{R}, for the applications discussed below we content ourselves with the assumption that

$$m = \hat{m}(c_{\mathrm{R}}). \tag{10.1}$$

In fact, following Baek and Srinivasa (2004) and Duda et al. (2010) we assume that the dependence of m on c_{R} is of a simple power-law form

$$m \propto c_{\mathrm{R}}^n, \tag{10.2}$$

16

with $n \geq 1$ a constant; this choice for the dependence of m on c_R models an increase in the mobility of fluid permeation as the polymer network is "opened" by an increase in the local fluid content.

Since the polymer volume fraction ϕ is dimensionless and is a comfortably-bounded quantity between zero and unity (cf. (8.2)),

$$\phi \stackrel{\text{def}}{=} (1 + vc_R)^{-1} \qquad \text{with} \qquad 0 < \phi \leq 1, \tag{10.3}$$

for the applications considered in this section we find it convenient to use ϕ rather than the fluid content c_R in the field equations (9.1) and (9.3).

Also, since

$$c_R \propto \left(\frac{1 - \phi}{\phi} \right), \tag{10.4}$$

instead of (10.1) and (10.2), we assume that

$$m = \hat{m}(\phi) = \frac{D}{vk_B\vartheta} \left(\frac{1 - \phi}{\phi} \right)^n, \tag{10.5}$$

where $D > 0$, a constant, represents a *permeability coefficient*.

Next, using (10.3) and the resulting relation

$$\dot{c}_R = -\frac{\dot{\phi}}{v\phi^2}, \tag{10.6}$$

the field equations (9.1), (9.2) (neglecting body forces), and (9.3) may be alternatively written as

$$\left. \begin{aligned} &\phi \det \mathbf{F} = 1, \\ &\mathrm{Div}\, \mathbf{T}_R = \mathbf{0}, \\ &\dot{\phi} = -v\phi^2 \mathrm{Div}\,(m\nabla\mu), \end{aligned} \right\} \tag{10.7}$$

with $\mathbf{T}_R$ given by (8.19), $m = \hat{m}(\phi)$ given by (10.5), and $\mu = \hat{\mu}(\phi)$ given by (8.22).

10.1 Isotropic stress-free equilibrium swelling

First, we consider the simple case of three-dimensional isotropic swelling-equilibrium of an elastomeric gel in a stress-free state. For isotropic swelling the deformation gradient $\mathbf{F}$ has the simple form

$$\mathbf{F}(\mathbf{X}, t) = \lambda(\mathbf{X}, t)\mathbf{1}, \tag{10.8}$$

and application of the swelling constraint $(10.7)_1$ gives

$$\lambda(\mathbf{X}, t) = \phi(\mathbf{X}, t)^{-1/3}. \tag{10.9}$$

Substituting (10.8) and (10.9) in eq. (8.19) for the stress, and using the fact that we are considering stress-free swelling, we have

$$G\phi^{-1/3}\mathbf{1} - P\phi^{1/3}\mathbf{1} = \mathbf{0}, \tag{10.10}$$

so that the field P is given by

$$P = G\phi^{-2/3}. \tag{10.11}$$

Use of (10.11) in (8.22) gives

$$\mu = \mu^0 + k_B\vartheta\left(\ln(1 - \phi) + \phi + \chi\phi^2 \right) + vG_0(\zeta\phi^{1/3} - \phi). \tag{10.12}$$

Swelling-equilibrium is attained when the chemical potential μ throughout the gel reaches the chemical potential μ^0 of the pure solvent surrounding the gel (Flory, 1953),

$$\mu = \mu^0. \tag{10.13}$$

Parameter	Gaussian	non-Gaussian
G_0	$0.1\,\text{MPa}$	$0.1\,\text{MPa}$
λ_L	$-$	2.5
υ	$1.7{\times}10^{-28}\,\text{m}^3$	$1.7{\times}10^{-28}\,\text{m}^3$
χ	0.1	0.1
μ^0	$0.0\,\text{J}$	$0.0\,\text{J}$

Table 1: Material parameters for a representative elastomeric gel.

Thus, from (10.12) the value of the polymer volume fraction after equilibrium has been attained, ϕ_e, may be determined by solving the implicit equation

$$k_B\vartheta\Big(\ln(1-\phi_e) + \phi_e + \chi\phi_e^2\Big) + \upsilon G_0(\zeta\phi_e^{1/3} - \phi_e) = 0, \tag{10.14}$$

and thence $\lambda_e = \phi_e^{-1/3}$, and also $J_e = \lambda_e^3$ may also be determined.

Table 1 lists plausible values for the material properties of a polymeric gel at room temperature, $20\,^\circ\text{C}$. Specifically, the ground state shear modulus for the polymer, G_0, is chosen to have a value $0.1\,\text{MPa}$, and the locking stretch parameter is taken to have a value $\lambda_L = 2.5$, so that the effects of chain-locking are easily observable when we compare results from a theory based on non-Gaussian statistics against results based on a theory which uses Gaussian statistics. The volume of a solvent molecule is taken as $\upsilon = 1.7 \times 10^{-28}\text{m}^3 \equiv 100.0\,\text{cm}^3/\text{mol}$. Additionally, we have chosen a value of $\chi = 0.1$ for the Flory-Huggins interaction parameter — a value which is favorable for a high degree of swelling. Using the material parameters in Table 1, solutions of (10.14) give

- **Case 1, Gaussian theory**:

$$\phi_e = 0.0566, \qquad \lambda_e = 2.6045, \qquad J_e = 17.667. \tag{10.15}$$

- **Case 2, non-Gaussian theory**:

$$\phi_e = 0.1552, \qquad \lambda_e = 1.8608, \qquad J_e = 6.44. \tag{10.16}$$

These results clearly show that the non-Gaussian theory, which accounts for the effects of limited chain extensibility, predicts a significantly smaller amount of swelling at equilibrium than the classical Gaussian-statistics-based theory.

Remark 3:
At a given temperature ϑ, the ground-state shear modulus $G_0 = N_{\text{R}}k_b\vartheta$ is proportional to the number of chains per unit reference volume, N_{R}, in an elastomer, and N_{R} itself is *directly proportional* to the degree of cross-linking (which determines the mean number of segments in a polymer chain connecting two neighboring junction points in an elastomer). In order to get a physical feel for how N_{R} and the χ-parameter affect the swelling behavior of a gel, consider the Gaussian theory ($\zeta = 1$), and a gel which shows a high degree of swelling ($\phi_e \ll 1$); under these circumstances, using the approximation $\ln(1 - \phi_e) \approx -\phi_e - \phi_e^2/2$, and neglecting the term ϕ_e as compared to $\phi_e^{1/3}$ in (10.14), one obtains

$$\phi_e \approx \left(\frac{\upsilon N_{\text{R}}}{\frac{1}{2} - \chi}\right)^{3/5}. \tag{10.17}$$

Thus,

- For a given value of $\chi < 1/2$, we find that $\phi_e \propto N_{\text{R}}^{3/5}$, and hence if the gel is made from a weakly crosslinked polymer so that N_{R} is small, then the equilibrium volume fraction of polymer ϕ_e is small, or the amount of swelling is large.

- Also, for a given value of N_R, as χ becomes much smaller than $1/2$, the value of ϕ_e decreases, and the amount of swelling increases. On the other hand, as $\chi \to \frac{1}{2}$, the amount of swelling decreases until the solvent and polymer network are no longer miscible with each other. On a cautionary note, a possible conclusion from (10.17) that χ must be less than $1/2$, is based on an approximative analysis; in actual applications one may encounter $\chi > \frac{1}{2}$ (cf., Section 10.4.)

10.2 One-dimensional transient swelling

Next, we consider the transient swelling of a gel in a one-dimensional setting. With respect to Figure 2, the one-dimensional reference body B is in the form of a cylinder of dry polymer with axis aligned with the $\mathbf{e}_1$-direction and of height H_0, placed in a rigid container. The reference body occupies the region $0 \leq X_1 \leq H_0$, and the polymer is in contact with the solvent at the surface $X_1 = H_0$, which is traction-free. The body is constrained in the lateral $\mathbf{e}_2$- and $\mathbf{e}_3$-directions, so that the motion of the body, as it absorbs the fluid and swells is, of the form

$$x_1 = \chi(X_1, t), \qquad x_2 = X_2, \qquad x_3 = X_3, \tag{10.18}$$

and the axial stretch is given by

$$\lambda = \lambda(X_1, t) \stackrel{\text{def}}{=} \frac{\partial \chi(X_1, t)}{\partial X_1}. \tag{10.19}$$

We assume that the displacement of the gel surface at $X_1 = 0$ is zero, and that all the walls of the container are frictionless and impermeable to fluid flow. Thus, the boundary conditions for displacement, tractions, and chemical potential in this problem are:

- On the surface $X_1 = 0$:

$$x_1 = X_1, \qquad -\nabla\mu \cdot \mathbf{e}_1 = 0. \tag{10.20}$$

- On the surface $X_1 = H_0$:

$$\mu = \mu^0, \qquad \mathbf{T}_R\mathbf{e}_1 = \mathbf{0}. \tag{10.21}$$

- On the lateral surfaces:

$$-\nabla\mu \cdot \mathbf{e}_2 = 0, \qquad -\nabla\mu \cdot \mathbf{e}_3 = 0, \qquad \mathbf{e}_1 \cdot (\mathbf{T}_R\mathbf{e}_2) = 0, \qquad \mathbf{e}_1 \cdot (\mathbf{T}_R\mathbf{e}_3) = 0. \tag{10.22}$$

From (10.18) and (10.19), the deformation gradient has the matrix representation

$$[\mathbf{F}] = \begin{bmatrix} \lambda & 0 & 0 \\ 0 & 1 & 0 \\ 0 & 0 & 1 \end{bmatrix}. \tag{10.23}$$

Thus $\det \mathbf{F} = \lambda$, and use of the field equation $(10.7)_1$ (the swelling constraint) gives $\phi\lambda = 1$, or equivalently that the polymer volume fraction is related to the axial stretch by the relation

$$\phi(X_1, t) = \lambda(X_1, t)^{-1}. \tag{10.24}$$

Next, recalling the relation (8.19) for the Piola stress, viz.

$$\mathbf{T}_R = G\mathbf{F} - P\mathbf{F}^{-\top}, \tag{10.25}$$

and using (10.23) and (10.24), we have that the pertinent components of the Piola stress are

$$\left. \begin{array}{l} (T_R)_{11} = G\phi^{-1} - P\phi, \\ (T_R)_{22} = G - P, \\ (T_R)_{33} = G - P. \end{array} \right\} \tag{10.26}$$

Further, the equation of equilibrium, $(10.7)_2$ gives the following non-trivial equilibrium equation to be satisfied

$$\frac{\partial}{\partial X_1}(G\phi^{-1} - P\phi) = 0; \tag{10.27}$$

19

which is satisfied, provided

$$G\phi^{-1} - P\phi = C, \tag{10.28}$$

with C independent of X_1.

Next, using $(10.26)_1$ and applying the traction-free boundary condition $\mathbf{T}_R\mathbf{e}_1 = \mathbf{0}$ at $X_1 = H_0$, requires that

$$(T_R)_{11}\Big|_{X_1=H_0} = \Big[G\phi^{-1} - P\phi\Big]_{X_1=H_0} = 0, \tag{10.29}$$

and thus, using (10.28), that also

$$C = 0.$$

Hence, from (10.28) we obtain that the field P is given by

$$P = G\phi^{-2}. \tag{10.30}$$

Use of (10.30) in (10.26) gives

$$\left.\begin{aligned} &(T_R)_{11} = 0, \\ &(T_R)_{22} = G(1 - \phi^{-2}) = -G(\lambda^2 - 1), \\ &(T_R)_{33} = G(1 - \phi^{-2}) = -G(\lambda^2 - 1). \end{aligned}\right\} \tag{10.31}$$

The stress field (10.31) satisfies the equation of equilibrium $(10.7)_2$ and the boundary conditions $(10.21)_2$, $(10.22)_3$, and $(10.22)_4$. Note that in the present case of swelling ($\lambda > 1$), (10.31) shows that the lateral stresses $(T_R)_{22}$ and $(T_R)_{33}$ are *compressive*.

Having satisfied the first two field equations $(10.7)_1$ and $(10.7)_2$, we turn our attention next to the remaining field equation $(10.7)_3$ for the transient swelling response of the gel. Recalling the relation (8.22) for the chemical potential, and substituting for P from (10.30), we have the following expression for the chemical potential in terms of the polymer volume fraction ϕ,

$$\mu = \mu^0 + k_B\vartheta\Big[\ln(1 - \phi) + \phi + \chi\phi^2\Big] + \upsilon G_0(\zeta\phi^{-1} - \phi), \tag{10.32}$$

with

$$\zeta = \hat{\zeta}(\phi) = \left(\frac{\lambda_L}{3\bar{\lambda}}\right)\mathcal{L}^{-1}\left(\frac{\bar{\lambda}}{\lambda_L}\right) \qquad \text{where} \qquad \bar{\lambda} = \frac{1}{\sqrt{3}}\sqrt{\phi^{-2} + 2}, \tag{10.33}$$

as defined before in $(8.16)_2$ and (8.5). Since the partial differential equation $(10.7)_3$ is phrased in terms of ϕ rather than μ, we next rewrite the initial and boundary conditions in terms of ϕ. Accordingly:

- The initial condition for the polymer volume fraction is

$$\phi(X_1, 0) = 1.0,$$

  so that at time $t = 0$ the reference body is a dry polymer.[10]

- The boundary condition for ϕ at the free surface $\phi(H_0, t)$ is denoted by ϕ_{H_0}, a time-invariant constant.[11] Therefore, using (10.32) we can determine ϕ_{H_0} by solving the implicit equation

$$k_B\vartheta\Big[\ln(1 - \phi_{H_0}) + \phi_{H_0} + \chi\phi_{H_0}^2\Big] + \upsilon G_0(\zeta_{H_0}\phi_{H_0}^{-1} - \phi_{H_0}) = 0, \tag{10.34}$$

  where $\zeta_{H_0} = \zeta(\phi_{H_0})$. Note that ϕ_{H_0} will also correspond to the *equilibrium value* of ϕ in the *whole body* as $t \to \infty$.

---

[10]In practice, we have used $\phi(X_1, 0) = 0.999$ rather than 1.0 to eliminate numerical difficulties with the $\ln(1 - \phi)$ term in (10.32). This approximation has no noticeable effect on the final numerical results.

[11]The boundary condition ϕ_{H_0} is time-invariant since, at time $t = 0$ the surface of the body is in contact with the solvent, and correspondingly, the chemical potential on the surface $X_1 = H_0$ is in equilibrium with that of the pure solvent, $\mu(X_1 = H_0, t) = \mu^0$.

- Since the flux in the $\mathbf{e}_1$-direction is

$$j = -\hat{m}(\phi)\frac{\partial\hat{\mu}(\phi)}{\partial X_1} = -\hat{m}(\phi)\frac{\partial\hat{\mu}(\phi)}{\partial\phi}\frac{\partial\phi}{\partial X_1}, \qquad (10.35)$$

the no-flux boundary condition $(10.20)_2$ is enforced by setting $\partial\phi/\partial X_1 = 0$ at $X_1 = 0$.

The partial differential equation $(10.7)_3$ with $m = \hat{m}(\phi)$ given by (10.5), $\mu = \hat{\mu}(\phi)$ given by (10.32) and (10.33), and the boundary conditions listed above, may be solved numerically for $\phi(X_1, t)$ using a finite-difference scheme. Details on our numerical solution procedure are given in an Appendix.

Parameter	Gaussian	non-Gaussian
G_0	$0.1\,\mathrm{MPa}$	$0.1\,\mathrm{MPa}$
λ_L	$-$	2.5
υ	$1.7\times10^{-28}\,\mathrm{m}^3$	$1.7\times10^{-28}\,\mathrm{m}^3$
D	$5.0\times10^{-9}\,\mathrm{m}^2/\mathrm{sec}$	$5.0\times10^{-9}\,\mathrm{m}^2/\mathrm{sec}$
n	1.0	1.0
χ	0.1	0.1
μ^0	$0.0\,\mathrm{J}$	$0.0\,\mathrm{J}$

Table 2: Parameters used in the transient swelling and squeezing problems.

The material parameters in our simulation for the transient free-swelling problem were chosen to be representative of a generic polymeric gel at room temperature, $20\,^\circ\mathrm{C}$, and are listed in Table 2. Values for the list $\{G_0, \lambda_L, \upsilon, \chi, \mu^0\}$ are taken from the previous example, and to that list we append the permeation-related parameters (D, n) for simulation of the transient response. We have chosen a value $D = 5.0\times10^{-9}\,\mathrm{m}^2/\mathrm{sec}$ for the permeability coefficient, and $n = 1$. The initial height of the dry polymer is taken as $H_0 = 0.01\,\mathrm{m}$.

- **Case 1**: We first consider results from simulations which use the material parameters listed in Table 2 for a free energy which neglects chain-locking, and uses Gaussian statistics to account for the change in entropy due to stretching.

  Figure 3a and Figure 3b, respectively, show plots of the polymer volume fraction ϕ and the axial stretch λ as functions of the normalized axial coordinate X_1/H_0 in the reference body, at different instances of time; the total time of our simulations is 24 hours. Figure 3a shows that the body begins as 100% polymer, and after 24 hours the top of the body ($X_1/H_0 = 1$) is only 19.97% polymer and 80.03% fluid, while the bottom of the body ($X_1/H_0 = 0$) is $\approx 30\%$ polymer and $\approx 70\%$ fluid. Note that we did not carry out our numerical simulations for periods of time which are long enough to have led to a situation of *equilibrium swelling*. At equilibrium the polymer volume fraction in the whole body is $\phi(\equiv \phi_{H_0}) = 0.1997$ (cf. (10.34)), and the corresponding equilibrium stretch is $\lambda = \phi^{-1} = 5.0075$; these equilibrium values are plotted as dashed lines in Figures 3a,b.

- **Case 2**: Next we consider results from simulations which use the material parameters listed in Table 2 for a theory which uses non-Gaussian statistics to account for the change in entropy due to stretching.

  Figure 4a and Figure 4b, respectively, show plots of the polymer volume fraction ϕ and the axial stretch λ as functions of the normalized axial coordinate X_1/H_0 in the reference body, at different instances of time; as before, the total time of our simulations is 24 hours. Figure 4a shows that the body begins as 100% polymer, and after 24 hours the top of the body ($X_1/H_0 = 1$) is 28.65% polymer and 71.35% fluid, while the bottom of the body ($X_1/H_0 = 0$) is $\approx 33\%$ polymer and $\approx 67\%$ fluid. Note that as before, we did not carry out our numerical simulations for periods of time which are long enough to have led to a situation of *equilibrium swelling*. At equilibrium, the polymer volume fraction in the whole body is $\phi(\equiv \phi_{H_0}) = 0.2865$ (cf. (10.34)), and the corresponding equilibrium stretch is $\lambda = \phi^{-1} = 3.49$; these equilibrium values are plotted as dashed lines in Figures 4a,b.

To provide a more physical picture of the swelling process, Figure 5 shows representative images of the time history of the *deformed body* during transient swelling; Figure 5a shows the results from numerical

21

simulations which use the Gaussian statistics-based theory, and Figure 5b shows the results from the non-Gaussian theory. At each time, the dashed rectangle represents the reference body, and the filled rectangle represents the deformed (swollen) body. Also shown plotted on the deformed body are contour plots of the polymer volume fraction ϕ. Note that at each of the times shown in Figure 5, the non-Gaussian theory exhibits a significantly smaller amount of swelling due to the effects of limited chain extensibility.

10.3   Squeezing/Consolidation of an initially swollen gel

Next we consider the gels from the previous example, which have been held long enough to have reached their "equilibrium" swollen configurations. Thus, using the equilibrium solutions from the previous example, the initial heights H_0 of the specimens are now taken as

$$\left.\begin{array}{ll} \bullet \ H_0 = 5.0075 \times 10^{-2}\,\mathrm{m}, & \text{for the Gaussian theory,} \\ \bullet \ H_0 = 3.4904 \times 10^{-2}\,\mathrm{m}, & \text{for the non-Gaussian theory,} \end{array}\right\} \tag{10.36}$$

and the initial conditions for the polymer volume fraction are taken as

$$\left.\begin{array}{ll} \bullet \ \phi(X_1, t = 0) = 0.1997, & \text{for the Gaussian theory,} \\ \bullet \ \phi(X_1, t = 0) = 0.2865, & \text{for the non-Gaussian theory.} \end{array}\right\} \tag{10.37}$$

In the problem studied here, these swollen gels are subjected to a compressive normal traction of magnitude S to the upper surface via a *permeable* plate; Figure 6 shows a schematic of the geometry and boundary conditions for the problem. Under the applied compressive normal traction S, we expect that the fluid *squeezes out* of the gel, so that the polymer volume fraction of the gel increases and height of the gel decreases, both as a function of relative position X_1/H_0 and time t.[12]

The boundary conditions for the displacements, tractions, and chemical potential for this example are:

- On the surface $X_1 = 0$:
$$x_1 = X_1, \quad -\nabla\mu \cdot \mathbf{e}_1 = 0, \tag{10.38}$$

- On the surface $X_1 = H_0$:
$$\mu = \mu^0, \quad \mathbf{T}_{\mathrm{R}}\mathbf{e}_1 = -S\mathbf{e}_1, \tag{10.39}$$

- On the lateral surfaces:
$$-\nabla\mu \cdot \mathbf{e}_2 = 0, \quad -\nabla\mu \cdot \mathbf{e}_3 = 0, \quad \mathbf{e}_1 \cdot (\mathbf{T}_{\mathrm{R}}\mathbf{e}_2) = 0, \quad \mathbf{e}_1 \cdot (\mathbf{T}_{\mathrm{R}}\mathbf{e}_3) = 0. \tag{10.40}$$

Mimicking the steps of the previous example, and accounting for the boundary condition $\mathbf{T}_{\mathrm{R}}\mathbf{e}_1 = -S\mathbf{e}_1$, we find that in this case
$$(T_{\mathrm{R}})_{11} = -S, \tag{10.41}$$

throughout the height of the gel (instead of $(T_{\mathrm{R}})_{11} = 0$), the scalar field P is now given by
$$P = G\phi^{-2} + S\phi^{-1}, \tag{10.42}$$

and the lateral stresses are given by
$$(T_{\mathrm{R}})_{22} = (T_{\mathrm{R}})_{33} = G(1 - \phi^{-2}) - S\phi^{-1}. \tag{10.43}$$

Also, use of (10.42) in (8.22) shows that the chemical potential inside the body given by
$$\mu = \mu^0 + k_B\vartheta\Big[\ln(1 - \phi) + \phi + \chi\phi^2\Big] + \upsilon G_0(\zeta\phi^{-1} - \phi) + \upsilon S, \tag{10.44}$$

with $\zeta = \hat{\zeta}(\phi)$ given in (10.33). As in the previous example,

---

[12]A similar problem was first analyzed by Terzaghi (1923,1943) in the context of one-dimensional linear poro-elasticity, and by Biot (1941) in the context of complete theory of linear poro-elasticity; the problem has also been recently analyzed by Hong et al. (2008) in the context of gels.

- The boundary condition for ϕ at the top surface is denoted by ϕ_{H_0}, and following arguments similar to those in the previous example, ϕ_{H_0} is determined by solving the implicit equation

$$k_B \vartheta \left[\ln(1 - \phi_{H_0}) + \phi_{H_0} + \chi \phi_{H_0}^2 \right] + \upsilon G_0 (\zeta_{H_0} \phi_{H_0}^{-1} - \phi_{H_0}) + \upsilon S = 0, \qquad (10.45)$$

where $\zeta_{H_0} = \hat{\zeta}(\phi_{H_0})$. Note that ϕ_{H_0} will also correspond to the *equilibrium value* of ϕ in the *whole body* as $t \to \infty$.

- The no-flux boundary condition $(10.38)_2$ is enforced by setting $\partial \phi / \partial X_1 = 0$ at $X_1 = 0$.

The field equation $(10.7)_3$ is solved numerically by using the same finite-difference procedure as in the previous example. The material parameters are taken to be the same as those used in the previous example, and given in Table 2. Further, we have used a compressive stress of $S = 3\,\mathrm{MPa}$.

- **Case 1**: As before, we first consider results from simulations which use the material parameters listed in Table 2 for a free energy which uses Gaussian statistics.

  Figure 7a and Figure 7b, respectively, show plots of the polymer volume fraction ϕ and the axial stretch λ as functions of the normalized axial coordinate X_1/H_0 in the reference body, at different instances of time; the total time of our simulations is 24 hours. Figure 7a shows that the body begins as 19.97% polymer, and after 24 hours the top of the body ($X_1/H_0 = 1$) is 45.38% polymer, while the bottom of the body ($X_1/H_0 = 0$) is $\approx 30\%$ polymer. As before, we did not carry out our numerical simulations for periods of time which are long enough to have led to an *equilibrium* situation. The equilibrium value of polymer volume fraction is $\phi(\equiv \phi_{H_0}) = 0.4538$ in the whole body, and the corresponding equilibrium stretch is $\lambda = 2.2036$; these equilibrium values are plotted as dashed lines in Figures 7a,b.

- **Case 2**: Next we consider results from simulations which use the material parameters listed in Table 2 for a free energy which uses non-Gaussian statistics.

  Figure 8a and Figure 8b , respectively, show plots of the polymer volume fraction ϕ and the axial stretch λ as functions of the normalized axial coordinate X_1/H_0 in the reference body, at different instances of time; as before, the total time of our simulations is 24 hours. Figure 8a shows that the body begins as 28.65% polymer, and after 24 hours the top of the body ($X_1/H_0 = 1$) is 45.82% polymer, while the bottom of the body ($X_1/H_0 = 0$) is $\approx 42\%$ polymer. The equilibrium value of polymer volume fraction is $\phi(\equiv \phi_{H_0}) = 0.4582$ in the whole body, and the corresponding equilibrium stretch is $\lambda = 2.1825$; these equilibrium values are plotted as dashed lines in Figures 8a,b.

The results clearly show that in both cases the fluid has been "squeezed" out of the body due to the applied compressive normal traction. Finally, to provide a more physical picture of the squeezing/consolidation process, Figure 9 shows representative images of the time history of the deformed bodies during transient consolidation; Figure 9a shows the results from numerical simulations which use the Gaussian statistics-based theory, and Figure 9b shows the results from the non-Gaussian statistics theory. At each of the times depicted in Figure 9 the dashed rectangle represents the initially swollen reference body, and the filled rectangle represents the deformed (squeezed) body. Also shown plotted on the deformed body are contour plots of the polymer volume fraction ϕ at the different instances of time.

10.4 Diffusion across a membrane

As a final example, we consider the problem of pressure-difference-driven diffusion of fluids across polymer membranes.[13] The specific problem discussed here is the transport of organic liquids through a highly-swollen rubbery membrane, a problem which has been experimentally studied by Paul and Ebra-Lima (1970). This problem has also been previously analyzed by Rajagopal (2003) (who used a mixture-theory approach), Baek and Srinisvasa (2004), and Duda et. al. (2010). The analysis presented here is a simplified version of the analysis presented by Duda et. al. (2010).

---

[13]Useful practical applications of such a phenomenon are encountered in diverse applications such as water purification — especially desalination by reverse osmosis.

Figure 10 shows a schematic of the geometry and boundary conditions for this problem: a gel of initial height H_0 is placed on a permeable plate on a container with frictionless rigid walls, and the top and bottom faces of the gel are subjected to pressures $p(X_1 = H_0, t) = p_{H_0}$ and $p(X_1 = 0, t) = p_0 = 0$, to obtain a pressure difference $\Delta p = p_{H_0} - p_0 \geq 0$ across the membrane. We analyze two situations:

- First we consider the transient response of the system.

- Next, we consider the steady-state response of the system, and compare our theoretical result for the steady-state flux as a function of the pressure difference against corresponding experimental data from Paul and Ebra-Lima (1970).

Since in this example the stretches are relatively small, we use only the theory based on Gaussian statistics.

10.4.1 Transient diffusion across a membrane

The boundary conditions for this problem are:

- On the surface $X_1 = 0$:
$$x_1 = X_1, \qquad \mu = \mu^0, \tag{10.46}$$

- On the surface $X_1 = H_0$:
$$\mathbf{T}_{\mathrm{R}}\mathbf{e}_1 = -p_{H_0}\mathbf{e}_1, \qquad \mu = \mu^0 + \upsilon p_{H_0}, \tag{10.47}$$

- On the lateral surfaces:
$$-\nabla\mu \cdot \mathbf{e}_2 = 0, \qquad -\nabla\mu \cdot \mathbf{e}_3 = 0, \qquad \mathbf{e}_1 \cdot (\mathbf{T}_{\mathrm{R}}\mathbf{e}_2) = 0, \qquad \mathbf{e}_1 \cdot (\mathbf{T}_{\mathrm{R}}\mathbf{e}_3) = 0. \tag{10.48}$$

Following a procedure similar to that in the previous examples, the state of stress inside the body is given by
$$\left.\begin{aligned}
(T_{\mathrm{R}})_{11} &= -p_{H_0} = -\Delta p, \\
(T_{\mathrm{R}})_{22} &= G_0(1 - \phi^{-2}) - \Delta p\, \phi^{-1}, \\
(T_{\mathrm{R}})_{33} &= G_0(1 - \phi^{-2}) - \Delta p\, \phi^{-1}.
\end{aligned}\right\} \tag{10.49}$$

Also, the chemical potential inside the body given by
$$\mu = \mu^0 + k_B\vartheta\left[\ln(1 - \phi) + \phi + \chi\phi^2\right] + \upsilon G_0(\phi^{-1} - \phi) + \upsilon\Delta p. \tag{10.50}$$

Since the partial differential equation $(10.7)_3$ is phrased in terms of ϕ rather than μ, we next rewrite the initial and boundary conditions in terms of ϕ:

- The reference body is taken to be a fully-dry polymer at the start of the simulation, so that ϕ obeys the initial condition
$$\phi(X_1, 0) = 1.0, \qquad 0 \leq X_1 \leq H_0. \tag{10.51}$$

- Since the body is in contact with the solvent at both surfaces $X_1 = 0$, and $X_1 = H_0$, we must prescribe boundary conditions $\phi = \phi_0$ at $X_1 = 0$, and $\phi = \phi_{H_0}$ at $X_1 = H_0$, respectively. These are obtained by solving the following set of implicit equations
$$k_B\vartheta\left[\ln(1 - \phi_0) + \phi_0 + \chi\phi_0^2\right] + \upsilon G_0(\phi_0^{-1} - \phi_0) + \upsilon\Delta p = 0 \qquad \text{at} \qquad X_1 = 0, \quad \text{and} \tag{10.52}$$
$$k_B\vartheta\left[\ln(1 - \phi_{H_0}) + \phi_{H_0} + \chi\phi_{H_0}^2\right] + \upsilon G_0(\phi_{H_0}^{-1} - \phi_{H_0}) = 0 \qquad \text{at} \qquad X_1 = H_0. \tag{10.53}$$

The field equation $(10.7)_3$ for the transient diffusion problem is solved numerically using the same finite-difference procedure used in the previous examples. The material parameters used in the numerical solution are those for natural gum rubber immersed in toluene listed in Table 3, and estimated from the experimental data of Paul and Ebra-Lima (1970). Further, we have used a pressure difference of $\Delta p = 500\,\mathrm{psi}$.

Parameter	Toluene	o-Xylene	iso-Octane
G_0, MPa	0.2669	0.2669	0.2669
v, m^3	1.8×10^{-28}	2.01×10^{-28}	2.81×10^{-28}
D, m^2/sec	1.3×10^{-9}	1.4×10^{-9}	0.9×10^{-9}
n	3	2	3
χ	0.425	0.408	0.572
μ^0, J	0.0	0.0	0.0

Table 3: Material parameters used in the pressure-difference-induced diffusion problem. The polymeric network is a cross-linked pure gum rubber, and the solvents are Toluene, o-Xylene, and iso-Octane. The initial thickness of the membrane is $H_0 = 0.0265$ cm and the temperature is $30\,^\circ$C. Data estimated from Paul and Ebra-Lima (1970).

Figure 11a and Figure 11b, respectively, show plots of the polymer volume fraction ϕ and the axial stretch λ as functions of the normalized axial coordinate X_1/H_0 in the reference body, at different instances of time; the arrows show increasing time, with the last curve shown in each figure almost at steady-state. Note that at steady-state the polymer volume fraction at the top of the gel is $\phi_{H_0} = 0.3576$, while that at the bottom of the gel is $\phi_0 = 0.6114$, and correspondingly the stretch at the top of the gel is $\lambda(X_1 = H_0, t) = 2.80$, while that at the bottom of the gel is $\lambda(X_1 = 0, t) = 1.64$.

10.4.2 Steady state diffusion across a membrane

At steady-state, the polymer volume fraction varies with X_1, as shown in Figure 11a. Presume that we have calculated ϕ_0 and ϕ_{H_0} for a given Δp. We now wish to calculate the steady-state flux of the fluid across the membrane.

Recall (10.35), viz.

$$j = -\hat{m}(\phi)\frac{\partial\hat{\mu}(\phi)}{\partial\phi}\frac{\partial\phi}{\partial X_1}. \tag{10.54}$$

With a function $g(\phi)$ defined by the relation

$$\frac{\partial g(\phi)}{\partial\phi} \overset{\text{def}}{=} \hat{m}(\phi)\frac{\partial\hat{\mu}(\phi)}{\partial\phi}, \tag{10.55}$$

we may write (10.54) as

$$j = -\frac{\partial g(\phi)}{\partial X_1}. \tag{10.56}$$

At *steady-state* the flux is constant, $j = j_{\text{ss}}$. Therefore integration of (10.56) between the limits $X_1 = 0$ and $X_1 = H_0$ gives[14]

$$j_{\text{ss}} H_0 = g(\phi_0) - g(\phi_{H_0}). \tag{10.57}$$

For $\hat{m}(\phi)$ and $\hat{\mu}(\phi)$, given by (10.5) and (8.22), respectively, (10.55) gives

$$\frac{\partial g(\phi)}{\partial\phi} = \frac{D}{v}\left(\frac{1-\phi}{\phi}\right)^n\left(1 + 2\chi\phi - \frac{1}{1-\phi}\right) - \frac{DG_0}{k_B\vartheta}\left(\frac{1-\phi}{\phi}\right)^n(1 + \phi^{-2}). \tag{10.58}$$

For a given positive *integer* value of n, (10.58) may be integrated to compute $g(\phi)$.[15] Then, since ϕ_0 and ϕ_{H_0} at steady-state are known for a membrane of initial thickness H_0 and a given Δp, (10.57) gives the resulting steady-state flux j_{ss}. The corresponding steady-state volumetric flux is $v j_{\text{ss}}$.[16] For a given elastomeric membrane and a given solvent, a curve of steady-state volumetric flux of solvent versus Δp may be computed by repeating the calculation procedure outlined above for several values of Δp.

---

[14]Cf., Duda et al (2010), eq. (100).

[15]We use the commercial software package Mathematica to symbolically perform this integration.

[16]Recall that the flux j_{ss} is the number of particles per unit area per unit time, and v the volume of a single solvent particle.

The solid lines in Figure 12 show steady-state volumetric solvent flux (in units of $cm^3/cm^2/day$) versus Δp (in psi) curves for three organic solvents — Toluene, o-Xylene and iso-Octane — across cross-linked gum-rubber membranes of thickness $H_0 = 0.0265\,cm$, at a temperature of 30°C. The material parameters used to produce these curves are listed in Table 3. The material parameters (D, n) were calibrated to fit the experimentally-measured steady-state flux versus Δp curves, while all other material parameters for the three membrane-solvent pairs were taken directly from Paul and Ebra-Lima (1970).[17] Also plotted in Figure 12 are corresponding data points for the steady-state flux versus driving pressure difference, measured experimentally by Paul and Ebra-Lima (1970). The theory nicely reproduces the highly nonlinear dependence of the flux on the driving-pressure for the three solvent-polymer combinations.

11   Concluding Remark

By viewing a fluid-solid mixture as a single, homogenized continuum body which allows for a mass flux of the fluid, we have developed a large-deformation theory to describe the various coupled aspects of fluid permeation and deformations of elastomeric gels. We have particularized the theory by considering a special free energy based on a Flory-Huggins model for the free energy change due to mixing of the fluid with the polymer network, coupled with a non-Gaussian statistical-mechanical model which accounts for the limited extensibility of polymer chains.

As representative simple examples of application of the theory, we have studied (a) isotropic three-dimensional swelling-equilibrium of an elastomeric gel in an unconstrained, stress-free state; and (b) the following one-dimensional transient problems: (i) free-swelling of a gel; (ii) consolidation of an already swollen gel; and (iii) pressure-difference-driven diffusion of organic solvents across elastomeric membranes.

In the future we plan to extend the theory to allow for mechanical (elastic) compressibility, and to implement such a theory in a full three-dimensional finite element program to solve general initial-boundary-value problems involving gels.

Acknowledgements

---

[17]Paul and Ebra-Lima (1970) studied the diffusion of several solvents across cross-linked natural gum-rubber membranes; we limit our attention here to the three solvents listed in Table 3.

References

Anand, L., 1996. A constitutive model for compressible elastomeric materials. Computational Mechanics 18, 339-355.

Anand, L., Gurtin, M.E., 2003. A theory of amorphous solids undergoing large deformations, with application to polymeric glasses. International Journal of Solids and Structures 40, 1465-1487.

Anand, L., Ames, N.M., Srivastava, V., Chester, S.A., 2009. A thermo-mechanically coupled theory for large deformations of amorphous polymers. Part I: Formulation. International Journal of Plasticity 25, 1474-1494.

Arruda, E.M., Boyce, M.C., 1993. A three-dimensional constitutive model for the large stretch behavior of rubber elastic materials. Journal of the Mechanics and Physics of Solids 41, 389-412.

Baek, S., Srinivasa, A.R., 2004. Diffusion through an elastic solid undergoing large deformation. Journal of Non-Linear Mechanics 39, 201-218.

Biot, M. A., 1941. General theory for three-dimensional consolidation. Journal of Applied Physics 12, 155-164.

Bischoff, J.E., Arruda, E.M., and Grosh, K., 2001. A new constitutive model for the compressibility of elastomers at finite deformations. Rubber Chemistry and Technology 74, 541-559.

Bowen, R.M., 1969. Thermochemistry of a reacting mixture of elastic materials with diffusion. Archive for Rational Mechanics and Analysis 34, 97-127.

Boyce, M.C., and Arruda E.M., 2001. Swelling and mechanical stretching of elastomeric materials. Mathematics and Mechanics of Solids 6, 641-659.

Cohen, A., 1991. A Padé approximant to the inverse Langevin function. Rheologica Acta 30, 270-273.

Doi, M., 1996. Introduction To Polymer Physics. Clarendon Press, Oxford.

Doi, M., 2009. Gel dynamics. Journal of the Physical Society of Japan 78, 052001.

Duda, F.P., Souza, A.C., and Fried, E., 2010. A theory for species migration in finitely strained solid with application to polymer network swelling. Journal of the Mechanics and Physics of Solids 58, 515-529.

Durning, C.J., and Morman, K.N., 1993. Nonlinear swelling of polymer gels. Journal of Chemical Physics 98, 4275-4293.

Flory, P.J., 1942. Thermodynamics of high polymer solutions. Journal of Chemical Physics 10, 51-61.

Flory, P.J., 1950. Statistical mechanics of swelling of network structures. Journal of Chemical Physics 18, 108-111.

Flory, P.J., 1953. Principles of polymer chemistry. Cornell University Press, Ithaca.

Fried, E., and Gurtin, M.E., 1999. Coherent solid-state phase transitions with atomic diffusion: a thermomechanical treatment. Journal of Statistical Physics 95, 1361-1427.

Fried, E., and Gurtin, M.E., 2004. A unified treatment of evolving interfaces accounting for deformation and atomic transport with emphasis on grain-boundaries and epitaxy. Advances in Applied Mechanics 40, 1-177.

Gurtin, M.E., 1996. Generalized Ginzburg-Landau and Chan-Hillard equations based on a microforce balance. Physica D 92, 178-192.

Gurtin, M.E., Fried, E., Anand, L., 2010. The Mechanics and Thermodynamics of Continua. Cambridge University Press, Cambridge.

Hong, W., Zhao, X., Zhou, J., and Suo, Z., 2008. A theory of coupled diffusion and large deformation in polymeric gel. Journal of the Mechanics and Physics of Solids 56, 1779-1793.

Huggins, M.L., 1942. Some properties of solutions of long-chain compounds. Journal of Physical Chemistry 46, 151-158.

Kröner, E., 1960. Allgemeine kontinuumstheorie der versetzungen und eigenspannungen. Archive for Rational Mechanics and Analysis 4, 273-334.

Lee, E.H., 1969. Elastic plastic deformation at finite strain. ASME Journal of Applied Mechanics 36, 1-6.

Lubarda, V.A., 2004. Constitutive theories based on the multiplicative decomposition of deformation gradient: thermoelasticity, elastoplasticity, and biomechanics. Applied Mechanics Reviews 57, 95-108.

Paul, K.R., Ebra-Lima, O.M., 1970. Pressure-induced diffusion of organic liquids through highly swollen polymer membranes. Journal of Applied Polymer Science 14, 2201-2224.

Podio-Guidugli, P., 2009. A virtual power format for thermomechanics. Continuum Mechanics and Thermodynamics 20, 479-487.

Rajagopal, K.R., 2003. Diffusion through polymeric solids undergoing large deformations. Materials Science and Technology 19, 1175-1180.

Tanaka, T., Fillmore, D.J., 1979. Kinetics of swelling of gels. Journal of Chemical Physics 70, 1214-1218.

Terzaghi, K., 1923. Die Berechnung des Durchlssigkeitsziffer des Tones aus dem Verlauf der hydrodynamischen Spannungserscheinungen. Sitz. Akad. Wiss. Wien, Abt. IIa 132, 125-138.

Terzaghi, K., 1943. Theoretical soil mechanics. Wiley, New York.

Treloar, L.R.G., 1975. The physics of rubber elasticity. Oxford University Press, Oxford.

Truesdell, C., 1984. Rational thermodynamics. Springer Verlag, New York.

Appendix: Numerical solution procedure

In this section we aim to provide the details of the numerical solution of the transient swelling example. The procedure used in the other examples is essentially the same with the exception of minor details such as boundary conditions. The partial differential equation for transient swelling is given by $(10.7)_3$ with $m = \hat{m}(\phi)$ given by (10.5), and $\mu = \hat{\mu}(\phi)$ given by (10.32). After some simplification $(10.7)_3$ may be written as

$$\dot{\phi} = \frac{D}{k_B \vartheta} \left[n \left(\frac{1-\phi}{\phi} \right)^{n-1} \frac{\partial \phi}{\partial X} \frac{\partial \mu}{\partial X} - \phi^2 \left(\frac{1-\phi}{\phi} \right)^n \frac{\partial^2 \mu}{\partial X^2} \right]. \tag{11.1}$$

We solve (11.1) numerically using a forward in time, centered space finite difference scheme. A one-dimensional grid is constructed of N points with uniform spacing h. We denote the time increment by a superscript k, and spatial location by a subscript i, where $X_1 = 0$ corresponds to $i = 1$, and $X_1 = H_0$ corresponds to $i = N$.

For the boundary condition at the top surface we have

$$\phi_N^k = \phi_{H_0}, \tag{11.2}$$

where ϕ_{H_0} is the prescribed boundary condition (see (10.34)). And for the no-flux condition at the bottom we have $\partial \phi / \partial X_1 = 0$, at $X_1 = 0$, which is satisfied when

$$\phi_1^k = \phi_2^k. \tag{11.3}$$

For the interior grid points we approximate the derivatives of ϕ with the finite-difference equations

$$\frac{\partial \phi}{\partial t} \approx \frac{\phi_i^{k+1} - \phi_i^k}{\Delta t}, \tag{11.4}$$

$$\frac{\partial \phi}{\partial X_1} \approx \frac{\phi_{i+1}^k - \phi_{i-1}^k}{2h}, \tag{11.5}$$

$$\frac{\partial^2 \phi}{\partial X_1^2} \approx \frac{\phi_{i+1}^k - 2\phi_i^k + \phi_{i-1}^k}{h^2}. \tag{11.6}$$

Also, at any given grid point, at any time increment, we can evaluate the chemical potential

$$\mu_i^k = \mu^0 + k_B \vartheta \left[\ln(1 - \phi_i^k) + \phi_i^k + \chi(\phi_i^k)^2 \right] + \upsilon G_0 \left(\zeta_i^k (\phi_i^k)^{-1} - \phi_i^k \right). \tag{11.7}$$

And we approximate derivatives of chemical potential with the finite-difference equations

$$\frac{\partial \mu}{\partial X} \approx \frac{\mu_{i+1}^k - \mu_{i-1}^k}{2h}, \tag{11.8}$$

$$\frac{\partial^2 \mu}{\partial X^2} \approx \frac{\mu_{i+1}^k - 2\mu_i^k + \mu_{i-1}^k}{h^2}. \tag{11.9}$$

The generalized shear modulus may also be computed at each grid point

$$G_i^k = G_0 \left(\frac{\lambda_L}{3\bar{\lambda}_i^k} \right) \mathcal{L}^{-1} \left(\frac{\bar{\lambda}_i^k}{\lambda_L} \right) = G_0 \zeta_i^k \tag{11.10}$$

with

$$\bar{\lambda}_i^k = \sqrt{\frac{(\phi_i^k)^{-2} + 2}{3}}. \tag{11.11}$$

It is important to note that the computation of $\mathcal{L}^{-1}(z)$ is not trivial. Cohen (1991) has developed a Padé approximation for the inverse Langevin function which we use in this work to greatly simplify the computation. Cohen's approximation is given by

$$\mathcal{L}^{-1}(z) \approx z \left(\frac{3 - z^2}{1 - z^2} \right) + \mathcal{O}(z^6).$$

This Padé approximation is much more accurate (preserving the limit as $\mathcal{L}^{-1}(z) \to \infty$ as $z \to 1$) and simple to implement than a high order series expansion.

With these approximations the discrete form of the field equation becomes

$$\dot{\phi}_i^k = \frac{D}{k_B \vartheta} \left[n \left(\frac{1 - \phi_i^k}{\phi_i^k} \right)^{n-1} \frac{\partial \phi}{\partial X} \frac{\partial \mu}{\partial X} - (\phi_i^k)^2 \left(\frac{1 - \phi_i^k}{\phi_i^k} \right)^n \frac{\partial^2 \mu}{\partial X^2} \right], \tag{11.12}$$

and values of ϕ at the grid points are updated in each time increment using

$$\phi_i^{k+1} = \phi_i^k + \Delta t \dot{\phi}_i^k. \tag{11.13}$$

Lastly, for this specific case, since information "flows" from the top surface down, the computational loop starts at $i = N$ and moves down the body to $i = 1$ in each time increment.
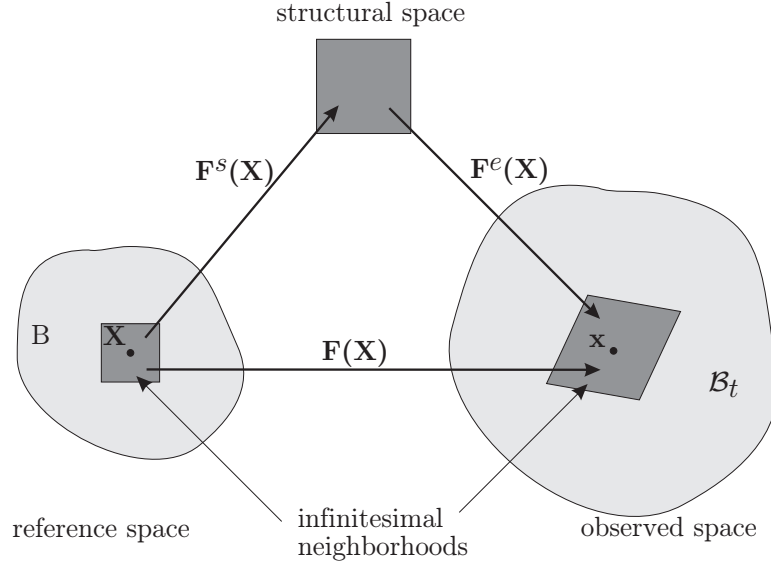
Figure 1: Schematic of the decomposition (2.2). The grey "boxes" denote infinitesimal neighborhoods of the points $\mathbf{X}$ in the reference body B, and $\mathbf{x} = \boldsymbol{\chi}(\mathbf{X}, t)$ in the deformed body $\mathcal{B}_t$. The arrows indicate the mapping properties of the linear transformations $\mathbf{F}$, $\mathbf{F}^s$, and $\mathbf{F}^e$.
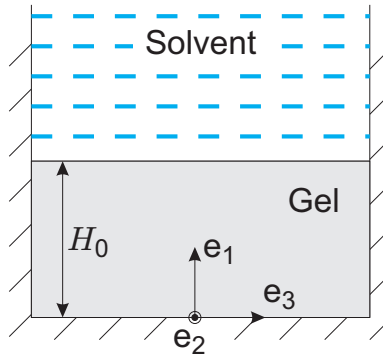

Figure 2: Schematic of the reference geometry of cylindrical polymer specimen in a rigid container used for the transient swelling problem. The gel is constrained from swelling in the $\mathbf{e}_2$- and $\mathbf{e}_3$-directions, and at the base $X_1 = 0$, the gel is fixed to the wall of the container. The walls of the container are assumed to be frictionless, and no fluid is allowed to diffuse through the walls.
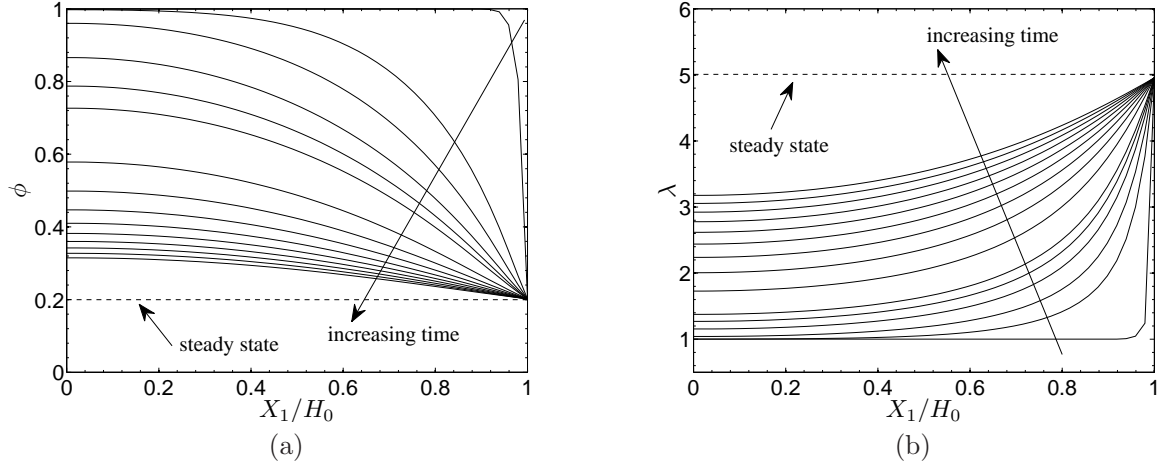
Figure 3: Transient swelling response of a gel using the Gaussian theory and the material parameters given in Table 2: (a) the polymer volume fraction ϕ, and (b) the axial stretch λ as a function of the normalized axial coordinate X_1/H_0 in the reference body at different instances of time, for a total time of 24 hours; the arrows indicate increasing time. The dashed lines indicate the steady-state values at time $t = \infty$.
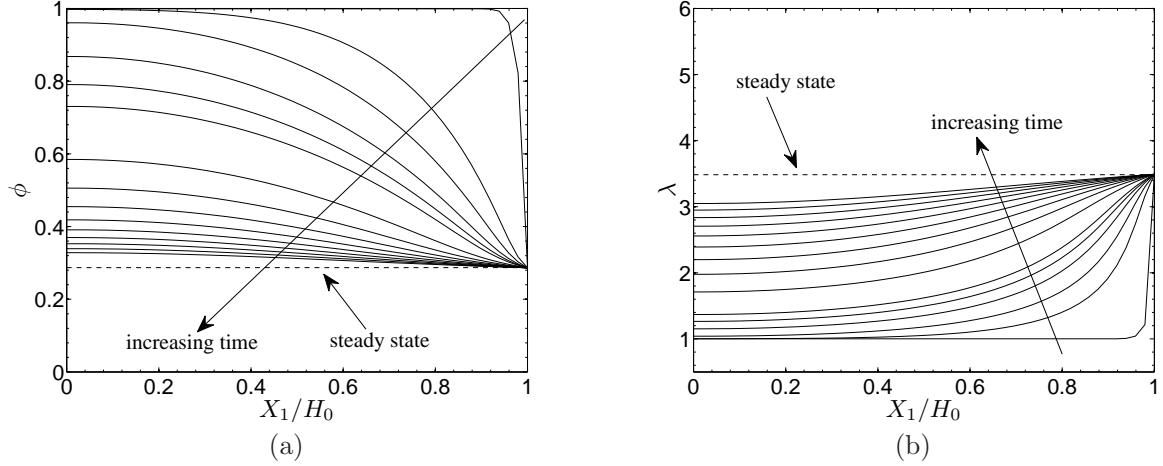

Figure 4: Transient swelling response of a gel using the non-Gaussian theory and the material parameters given in Table 2: (a) the polymer volume fraction ϕ, and (b) the axial stretch λ as a function of the normalized axial coordinate X_1/H_0 in the reference body at different instances of time, for a total time of 24 hours; the arrows indicate increasing time. The dashed lines indicate the steady-state values at time $t = \infty$.

31
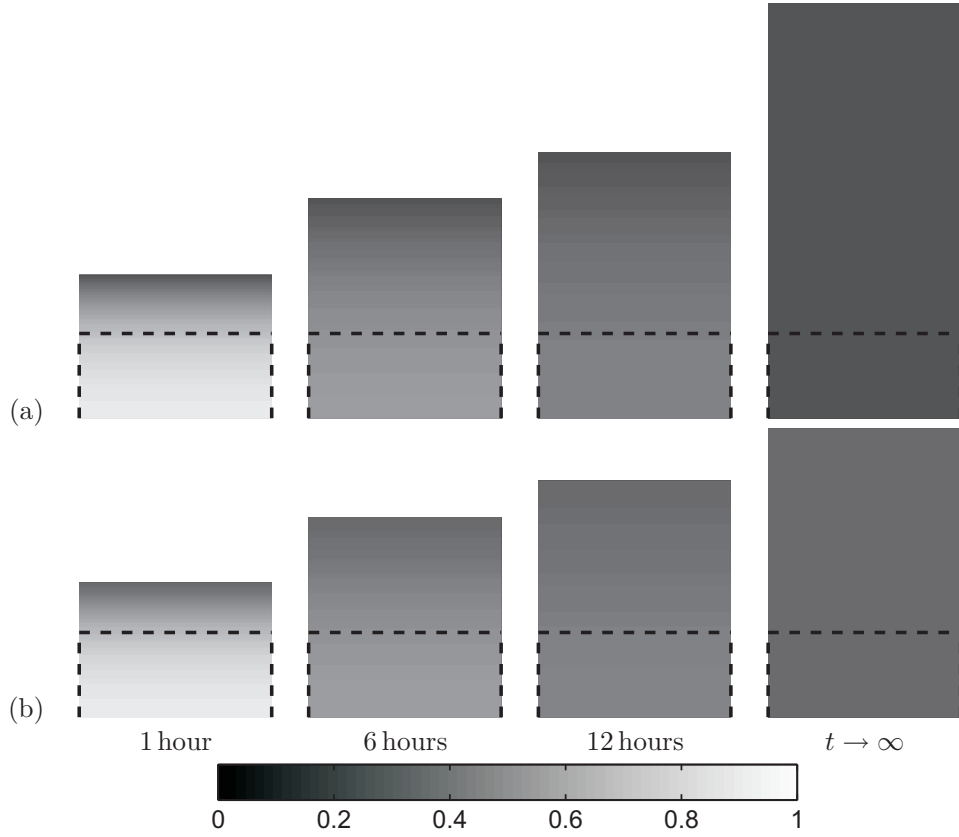
Figure 5: Representative images of the time history of the deformed body during transient swelling. At each time the dashed rectangle represents the reference body, and the filled rectangle represents the deformed (swollen) body. Also shown plotted on the deformed body are contour plots of the polymer volume fraction, ϕ, at different instances of time; the gray-scale bar gives numerical values of $0 \leq \phi \leq 1$: (a) Shows the results from numerical simulations which use the Gaussian theory, and (b) shows the results from the non-Gaussian theory. Note that at each time the non-Gaussian theory shows significantly smaller amount of swelling due to the effects of limited chain extensibility.
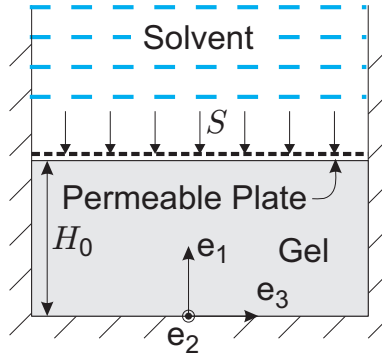
Figure 6: Schematic of the reference geometry of cylindrical fully-swollen gel specimen in a rigid container used for the transient squeezing problem. The gel is constrained from changing dimensions in the $\mathbf{e}_2$- and $\mathbf{e}_3$-directions, and at the base, $X_1 = 0$, the gel is fixed to the wall of the container. The walls of the container are assumed to be frictionless, and no fluid is allowed to diffuse through the walls. However, at the upper surface $X_1 = H_0$, a compressive normal traction $-S\mathbf{e}_1$ is applied, and fluid may squeeze out through a rigid permeable plate.
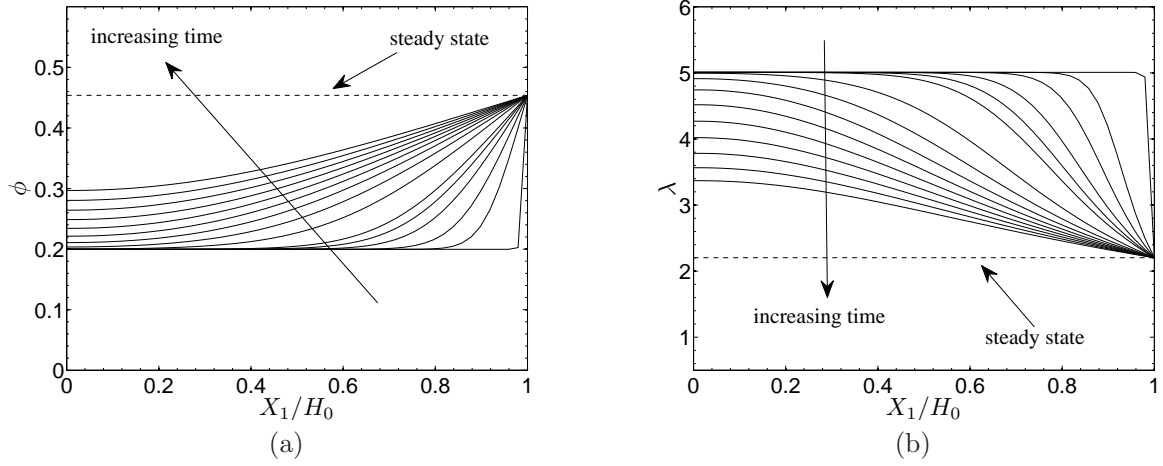
32

Figure 7: Transient squeezing response of a gel using the Gaussian theory and the material parameters given in Table 2: (a) the polymer volume fraction ϕ, and (b) the axial stretch λ as a function of the normalized axial coordinate X_1/H_0 in the reference body at different instances of time, for a total time of 24 hours; the arrows indicate increasing time. The dashed lines indicate the steady-state values at time $t = \infty$.
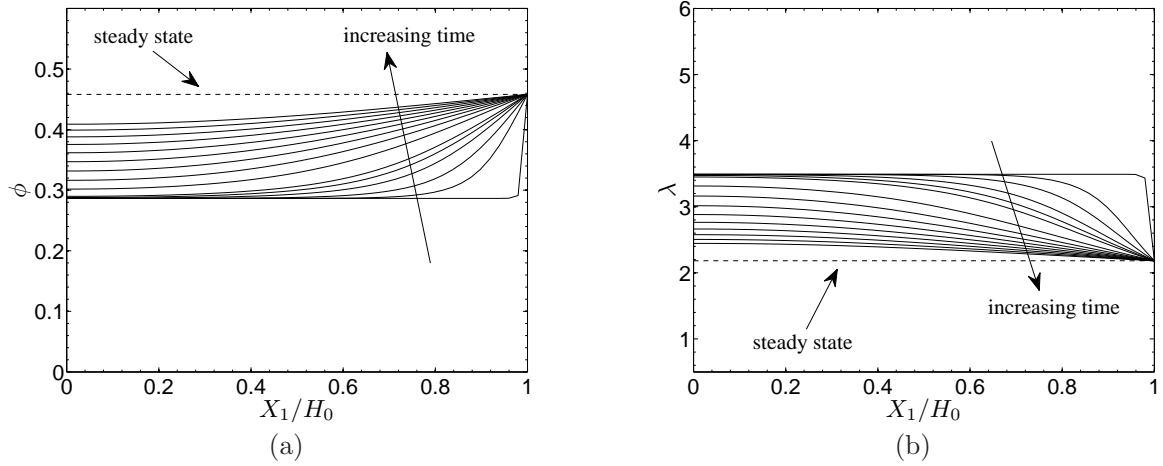

Figure 8: Transient squeezing response of a gel using the non-Gaussian theory and the material parameters given in Table 2: (a) the polymer volume fraction ϕ, and (b) the axial stretch λ as a function of the normalized axial coordinate X_1/H_0 in the reference body at different instances of time, for a total time of 24 hours; the arrows indicate increasing time. The dashed lines indicate the steady-state values at time $t = \infty$.
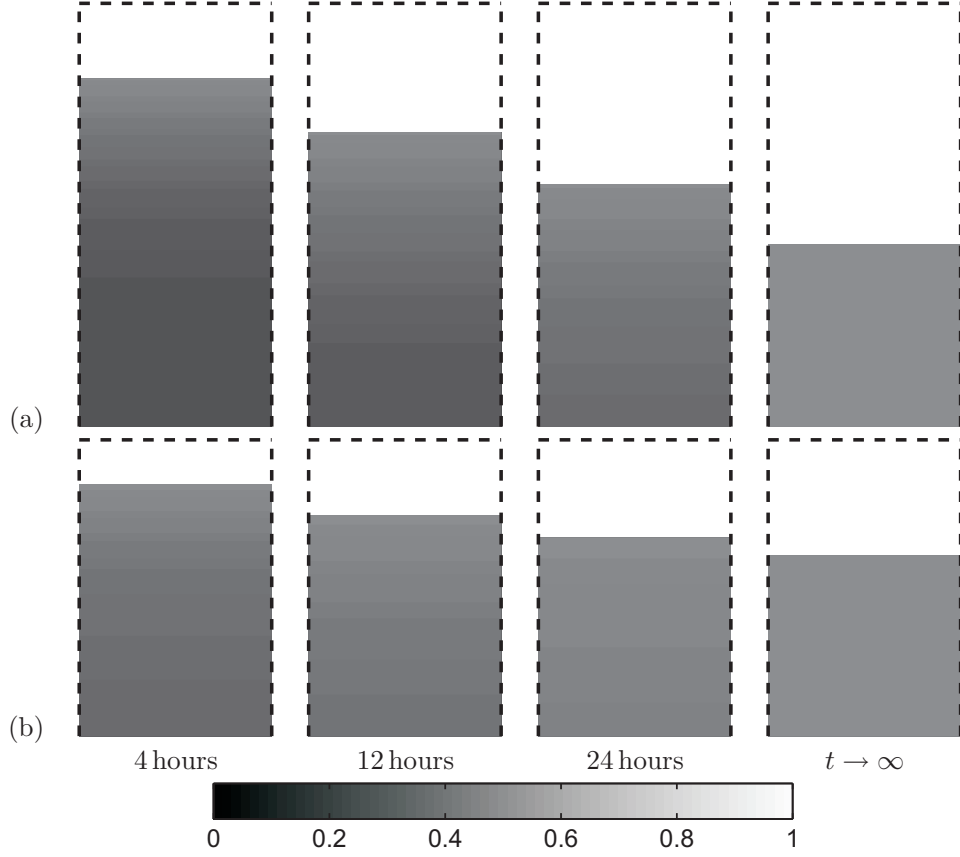
Figure 9: Representative images of the time history of the deformed body during transient squeezing/consolidation. At each time the dashed rectangle represents the reference body, and the filled rectangle represents the deformed (squeezed) body. Also shown plotted on the deformed body are contour plots of the polymer volume fraction ϕ at different instances of time; the gray-scale bar gives numerical values of $0 \leq \phi \leq 1$: (a) Shows the results from numerical simulations which use the Gaussian theory, and (b) shows the results from the non-Gaussian theory.
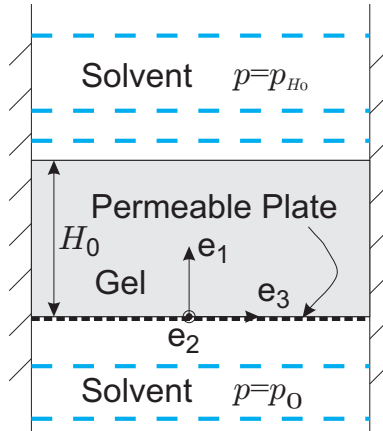

Figure 10: Schematic of the geometry used for the analysis of pressure-difference-driven diffusion across a polymer membrane. The gel is constrained from swelling in the $\mathbf{e}_2$- and $\mathbf{e}_3$-directions. At the base, $X_1 = 0$ the gel is fixed to a permeable plate so that fluid may pass through. A pressure difference $\Delta p = p_{H_0} - p_0 \geq 0$ is applied across the membrane to drive the fluid flux.

34

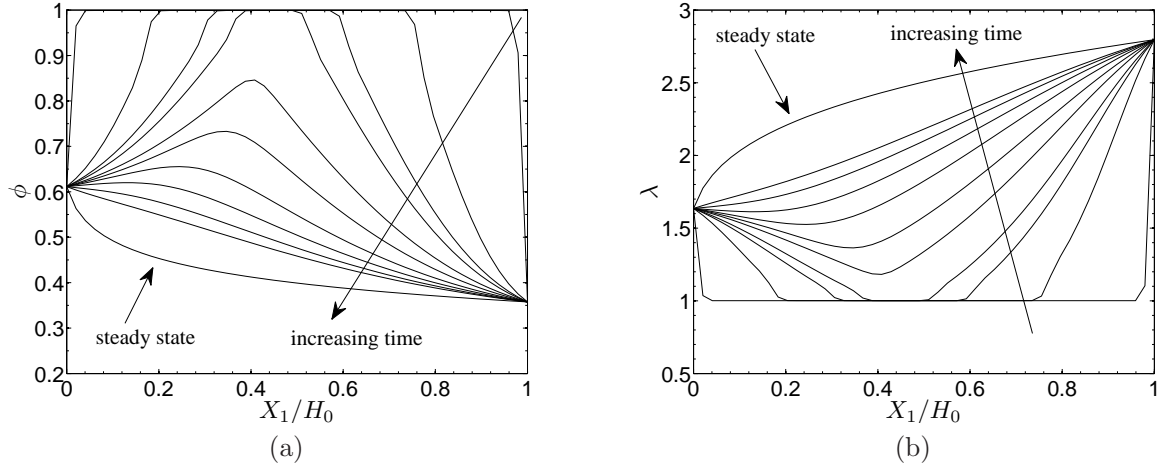(a)   (b)

Figure 11: Inhomogeneous transient response of (a) the polymer volume fraction and (b) the stretch in the pressure-driven-diffusion process for an applied Δp=500 psi. The arrows indicate increasing time, with the last curve shown corresponding to $||\dot{\phi}||_2 \leq 5 \times 10^{-5} s^{-1}$ (a small value) so that this curve corresponds to steady-state.
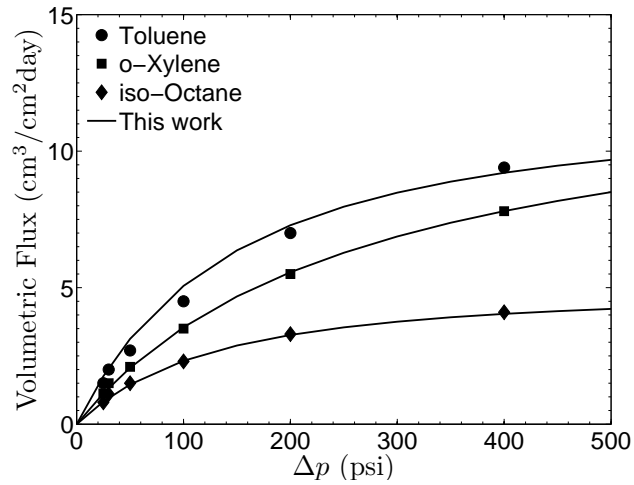

Figure 12: Comparison between numerically-calculated steady-state volumetric flux versus pressure-difference curves and corresponding experimental data from Paul and Ebra-Lima (1970).